OPTIMISATION OF CORONA RING DESIGN AND ITS IMPACT ON THE PERFORMANCE OF INSULATOR STRING IN HIGH VOLTAGE TRANSMISSION LINES

KALAISELVI A/P ARAMUGAM

FACULTY OF ENGINEERING
UNIVERSITY OF MALAYA
KUALA LUMPUR

2022

OPTIMISATION OF CORONA RING DESIGN AND ITS IMPACT ON THE PERFORMANCE OF INSULATOR STRING IN HIGH VOLTAGE TRANSMISSION LINES

KALAISELVI A/P ARAMUGAM

THESIS SUBMITTED IN FULFILMENT OF THE REQUIREMENTS FOR THE DEGREE OF DOCTOR OF PHILOSOPHY

FACULTY OF ENGINEERING
UNIVERSITY OF MALAYA
KUALA LUMPUR

2022

UNIVERSITY OF MALAYA
ORIGINAL LITERARY WORK DECLARATION

Name of Candidate: Kalaiselvi a/p Aramugam

Registration/Matric No: 17018953/3 (KHA 140043)

Name of Degree: Doctor of Philosophy

Title of Project Paper/Research Report/Dissertation/Thesis ("this Work"):

Optimisation of corona ring design and its impact on the performance of insulator string in high voltage transmission lines

Field of Study: High Voltage Engineering

I do solemnly and sincerely declare that:

(1) I am the sole author/writer of this Work;
(2) This Work is original;
(3) Any use of any work in which copyright exists was done by way of fair dealing and for permitted purposes and any excerpt or extract from, or reference to or reproduction of any copyright work has been disclosed expressly and sufficiently and the title of the Work and its authorship have been acknowledged in this Work;
(4) I do not have any actual knowledge nor do I ought reasonably to know that the making of this work constitutes an infringement of any copyright work;
(5) I hereby assign all and every rights in the copyright to this Work to the University of Malaya ("UM"), who henceforth shall be owner of the copyright in this Work and that any reproduction or use in any form or by any means whatsoever is prohibited without the written consent of UM having been first had and obtained;
(6) I am fully aware that if in the course of making this Work I have infringed any copyright whether intentionally or otherwise, I may be subject to legal action or any other action as may be determined by UM.

Candidate's Signature   Date: 23rd May 2022

Subscribed and solemnly declared before,

Witness's Signature   Date: 7 June 2022

Name:

Designation

OPTIMISATION OF CORONA RING DESIGN AND ITS IMPACT ON THE PERFORMANCE OF INSULATOR STRING IN HIGH VOLTAGE TRANSMISSION LINES

ABSTRACT

Installation of a corona ring on an insulator string on a transmission line is one of the solutions to reduce the electric field stress surrounding the energised end of the insulator string. However, installing a corona ring with an optimum design to reduce the electric field magnitude on an insulator string is a challenging task. Therefore, in this work, a method to achieve an optimum design of a corona ring for a 33 kV and 132 kV composite non-ceramic insulator string was proposed using optimisation methods; Gravitational Search Algorithm (GSA), Imperialist Competitive Algorithm (ICA) and Grey Wolf Optimisation (GWO). The composite non-ceramic insulator string geometry with and without corona ring was modeled in finite element analysis and used to obtain the electric field distribution in the model geometry. The electric field distribution was evaluated using variation of corona ring dimensions, i.e. the ring diameter, the ring tube diameter and the vertical position of the ring along the insulator string. From the results achieved, comparison of the minimum electric field magnitude along the insulator string with a corona ring design shows that the minimum electric field magnitude is lower using optimisation techniques. Among the methods tested, the most suitable technique is found based on insulator model used in this work. Hence, this indicates the capability and effectiveness of the proposed methods in achieving an optimum design of a corona ring on an insulator string.

Keywords: Insulator strings; optimisation techniques; high voltage engineering; transmission lines; corona rings

PENGOPTIMALKAN REKA BENTUK CINCIN CORONA DAN KESANNYA TERHADAP PRESTASI TENTENG PENEBAT DALAM TALIAN PENGHANTARAN VOLTAN TINGGI

ABSTRAK

Pemasangan cincin korona pada tali penebat pada saluran penghantaran adalah salah satu daripada penyelesaian untuk mengurangkan tegangan medan elektrik di sekitar hujung tali penebat yang diaktifkan. Walau bagaimanapun, memasang cincin korona dengan reka bentuk yang optimum untuk mengurangkan magnitud medan elektrik pada rentetan penebat adalah tugas yang mencabar. Oleh itu, dalam kerja ini, satu kaedah untuk mencapai reka bentuk optimum cincin korona untuk tali penebat bukan seramik komposit 33 kV dan 132 kV telah dicadangkan menggunakan kaedah pengoptimuman; Algoritma Pencarian Graviti (GSA), Algoritma Persaingan Imperialis dan Pengoptimuman Serigala Kelabu (GWO). Model geometri rentetan penebat bukan seramik komposit dengan cincin corona dan tanpa cincin korona dimodelkan dalam perisian analisis unsur terhingga dan digunakan untuk mendapatkan pengagihan medan elektrik dalam model geometri. Pengagihan medan elektrik dinilai menggunakan variasi dimensi cincin korona, iaitu diameter lingkaran, diameter tiub cincin dan kedudukan menegak cincin di sepanjang rentetan penebat. Daripada hasil yang dicapai, perbandingan magnitud medan elektrik minimum di sepanjang rentetan penebat dengan reka bentuk cincin korona menunjukkan bahawa magnitud medan elektrik minimum lebih rendah menggunakan teknik pengoptimuman. Antara kaedah yang diuji, teknik yang paling sesuai didapati berdasarkan model penebat yang digunakan dalam kerja ini.. Oleh itu, ini menunjukkan kaedah keupayaan dan keberkesanan yang dicadangkan untuk mencapai reka bentuk optimum cincin korona pada rentetan penebat.

Kata kunci: Tali penebat; teknik pengoptimuman; kejuruteraan voltan tinggi; talian penghantaran; cincin corona

ACKNOWLEDGEMENTS

TABLE OF CONTENTS

LIST OF FIGURES

LIST OF TABLES

LIST OF SYMBOLS AND ABBREVIATIONS

σ : Electrical conductivity (S/m)

ρ : Density of the material (kg/m3)

k : Thermal conductivity (W/mK)

$\mathcal{E}o$: Permittivity in vacuum

$\mathcal{E}r$: Relative permittivity of the material

C_p : Specific heat capacity of the material (J)

D_1 & D_2 : Electric displacement

E : Electric field (kV)

F : Frequency of the applied voltage (Hz)

H : Height of the ring along the insulator (mm)

I : Current (A)

J : Current density (A)

r : Ring tube diameter (mm)

R : Ring diameter (mm)

V : Electric potential (kV)

AC : Alternating Current

ACO : Ant Colony Optimisation

AI : Artificial Intelligence

BEM Boundary Element Method

CSM : Charge Simulation Method

EFVD : Electric Field Voltage Distribution

FEA : Finite Element Analysis

FEM	:	Finite Element Method
FDM	:	Finite Different Method
FRP	:	Fiberglass Reinforced Polymer
GSA	:	Gravitational Search Algorithm
GWO	:	Grey Wolf Optimisation
ICA	:	Imperialist Competitive Algorithm
PD	:	Partial Discharge
2D	:	Two dimension
3D	:	Three dimension

CHAPTER 1: INTRODUCTION

1.1 Overview

Insulator strings are widely used in high voltage transmission lines. Insulator strings are used to mechanically support the transmission conductor lines and as the electrical insulator between lines and the towers to reduce the discharge of the current that flows from conductor to earth. Electric field modeling is largely utilised in high voltage engineering, including for outdoor insulation. In recent years, extra high voltage power lines have been used to send electric energy from the power stations to the consumers. The electric field distribution on insulator strings along high voltage transmissions lines affects both long- and short-term performance. Insulators are the most important devices used for the suspension of overhead transmission lines because flashover can affect the insulators. Most of the high voltage insulators are designed with a lower flashover voltage than a puncture voltage, hence, flashover occurs before the puncture to avoid the damage. Insulation failure and loss of hydrophobicity could occur when the surface of the insulator is exposed to extremely high electric fields.

Corona phenomenon may cause a failure in the insulators due to the high intensity electric field. The crucial problem faced by outdoor insulators in high voltage is Partial discharge (PD). PD leads to extremely high electric field stress along the insulator surface or insulator ends. The insulator surface pollution is the cause of PD on the insulator surface. Therefore, both ends of an insulator are affected by PD activities and as a result of improper design of corona ring (Murawwi & El-Hag, 2011; Weiguo & Sebo, 2001). All these problems occur due to the non-uniform distribution of electric field along the insulator. Uneven electric field distribution tends to increase the electric field magnitude near to the phase terminal.

1

A fundamental knowledge and understanding of electric field distribution and the effect on the insulator performance is needed in order to design and apply composite insulators effectively (Diako Azizi, 2012). The calculation of electric field is very important to reduce the size and enhance the space utilisation efficiency. Therefore, fixing a corona ring on the insulator string is an effective way to minimise the electric field on the insulator string and decrease the effect of corona.

However, the optimisation of corona ring designs is still an active research interest since optimal dimensions produce the best reduction of the maximum electric field. Therefore, in this work, the optimisation of corona ring designs to reduce the electric field at the insulator string is performed using latest optimisation techniques, which include Imperialist Competitive Algorithm (ICA), Gravitational Search Algorithm (GSA) and Grey Wolf Optimisation (GWO). The methods of this work are compared with the existing published work to show the superiority of the work. The impact of the optimised corona ring designs on the performance of insulator string in high voltage transmission line is analysed and evaluated.

1.2   Problem Statement

In recent years, composite insulators are widely used in high voltage engineering since there are many advantages compared to other types of insulator. However, composite insulators still have to compete with ceramic and glass insulators, which have longer service life. The age of composite insulators and their lifetime is dependent upon the environmental conditions, especially the temperature variations and mainly on the magnitudes of electric field they are exposed to. Thus, the modeling of insulator is essential in serve better understanding of distribution of electric field along the surface of insulators.

The distribution of electric field along the insulator string is normally not uniform. This uneven distribution is affected by the conductor and coupling capacitors to extent, where mostly can be seen on the first and second insulations unit. This non-uniform distribution approximately 3 to 4 times more than other insulators units. Thus, the probability of corona phenomenon is higher, which may lead to complete failure of the insulation. Therefore, installing a corona ring together with insulator string is an effective method to minimise the distribution of electric field.

To enhance the power system reliability, compatibility and safety, it is required to have a good quality of material and increase their lifetime. This can be done by proper design and maintenance of corona ring and insulator. Improvement on reducing the electric field along the insulator under normal condition is still needed. All these requirements can be fulfilled by using numerical technique such as finite element analysis (FEA), which allows the researchers to develop an insulator model with corona ring based on the real physical dimensions. Therefore, the developed FEA model can be used to evaluate the factors that minimise the distribution of electric field along the insulator.

Although many studies related to distribution of electric field on insulator have been performed since the past, research works to reduce the electric field along insulator using optimisation methods are less likely to be found in literature. For this reason, the developed FEA models were interfaced with MATLAB programming code to obtain the optimised corona ring in minimising the distribution of electric field along the insulator by using optimization methods. This study focuses on optimisation of dimensions of corona ring using imperialist competitive algorithm (ICA), gravitational search algorithm (GSA) and grey wolf optimisation (GWO).

1.3 Objectives

In this work, the simulation of corona ring design and insulator string is performed under various ring dimensions and the design of corona ring was optimised by in order to reduce the electric field distribution along the insulator string. The main objectives of the work are:

1. To design a corona ring for non-ceramic insulator string using finite element analysis software

2. To investigate the electric field distribution in the model that has been developed under various corona ring dimensions

3. To propose optimum corona ring design for insulator string models based on optimisation algorithms

4. To evaluate a suitable optimisation algorithm for designing optimum corona ring of insulator string through comparison among different techniques

1.4 Scope of Study

The main use of a corona ring is to reduce electric field along an insulator string. Fixing a corona ring along the insulator string is an effective way to minimise the effect of electric field. However, optimum dimensions of corona ring are important so that the electric field magnitude can be reduced significantly. Hence, the main aim of this work is to design optimum dimensions of corona ring for insulator string models. A three-dimensional (3D) 33 kV insulator model with corona ring and a two-dimensional (2D) 132 kV insulator model with corona ring were developed using finite element analysis method to simulate the distribution of the electric field along the surface of an insulator. The developed FEA model was used to study the electric field with varying the dimensions of corona ring.

Basically, the difference between the 3D and 2D in FEA is they have different movement and deformation possibilities in the model. The length of the insulator model is the main reason to use both elements. 2D model is faster and easy to build and it was selected for 132 kV which has 40 weather sheds. While 3D model was selected for 33 kV with 10 weather sheds since its take time to compute the model and complicated in building up the model.

In order to validate the results, the results were compared with the existing published works. Then, the developed model was used to find the optimised dimensions of corona ring in reducing the electric field along insulator string. The main advantage of using optimisation methods is the best solutions can be obtained within shorter time. The optimisation techniques used to optimise the design are Imperialist Competitive Algorithm (ICA), Gravitational Search Algorithm (GSA) and Grey Wolf Optimisation (GWO). The results from these techniques were used in the FEA model to redesign the corona ring. In this work, electric field was evaluated based on the position of corona ring. Therefore, other atmospheric factors such as pollution and surface moisture is not considered. Through this work, a better understanding of minimum electric field distribution along insulator string can be attained, which may help the performance of insulator string in high voltage transmission lines.

1.5 Contributions of the Thesis

The contributions of the thesis are:

1. Works on reducing electric field distribution along insulator string were performed.

PD is the serious problems faced by outdoor insulators in high voltage. PD produces extremely high electric field stress along the insulator surface or insulator ends and it is cause of surface pollution. PD activities at both ends of an insulator are the main reason of not proper design of its corona ring. Therefore, by reducing the electric field using optimisation techniques, optimum corona ring design can be identified.

2. Modelling of a corona ring with insulator string under various dimensions were performed.

Designing a corona ring with insulator string using various dimensions was performed in this work. The optimisation of corona ring design produces the best reduction of the maximum electric field. Therefore, fixing a corona ring along the insulator string is an effective way to minimise the electric field on the insulator string and reduce the effect of corona. The calculation of electric field is also important to reduce the size and enhance utilisation efficiency.

3. Corona ring design was optimised to reduce electric field using optimisation methods

The developed model of corona ring with insulator using FEA method was used to optimise the corona ring design by interfacing the model with a MATLAB programming code. In this work, optimisation of corona ring designs to reduce the electric field at the insulator string is performed using recent optimisation techniques, which are Imperialist Competitive Algorithm (ICA), Gravitational Search Algorithm (GSA) and Grey Wolf Optimisation (GWO). No research has been undertaken in designing corona ring with insulator string using these algorithms. The impact of the optimised corona ring design on the performance of insulator string in high voltage transmission line is analysed and evaluated.

1.6   Outline of Thesis

This thesis is organised into five chapters as follows:

Chapter 1 is the introduction section. In this chapter, overview of corona ring design and non-ceramic insulators in high voltage transmission lines are briefly explained. At the end of this chapter, the objectives of the study and the thesis outline are stated.

Chapter 2 is the literature review section. This chapter contains explanation on ways to minimise the distribution of electric field along the non-ceramic insulators. Moreover, this chapter includes literature review on previous works that are related to the insulator string with corona ring and optimisation methods used to design corona ring dimensions.

Chapter 3 is the methodology section. In this section, the models developed in finite element analysis (FEA) describes in detail. Also, contains explanation the corona ring dimensions and the optimisation methods used in this work, which are imperialist competitive algorithm (ICA), gravitational search algorithm (GSA) and Grey Wolf Optimisation (GWO).

Chapter 4 is the results and discussion section. The results of the models with various dimensions are presented and discussed in this chapter. The parameters of the corona ring that influence the performance of electric field in insulator are analysed and explained. The optimised design of the corona ring based on ICA, GSA and GWO are also presented in this section.

Chapter 5 consists of conclusions and recommendation for future work. Conclusions are made based on the findings of the work and some recommendations are listed for future work.

CHAPTER 2: LITERATURE REVIEW

2.1 Introduction

This chapter discusses the types and structures of insulators, corona ring design, parameters of the corona ring, distribution of electric field and distribution of electric potential. Literature review related to non-ceramic insulator string and corona ring design is included. Also, corona ring and its role to minimise the distribution of electric field along the surface of the insulators are reviewed. A brief description and introduction to COMSOL Multiphysics and optimisation techniques are included. At the end of this chapter, research studies related to the distribution of electric field in non-ceramic insulators are reviewed.

2.2 Non-Ceramic Insulator String

Mainly in power system network the insulator strings are used for two different purposes which are mechanical support and electrical insulator between the live phase conductors and the support tower (Murawwi & El-Hag, 2011). In the earlier stage, line insulators are produced by using high quality glaze porcelain and toughened glass because these materials are known for its reliable factor and cost effective for a majority of outdoor applications. Later, an alternative material was found, which is polymer. Composite insulators are widely applied in both transmission and distribution voltage ranges and are steadily conquering a broader share in the market. Figure 2.1 shows the basic components of high voltage insulator string.
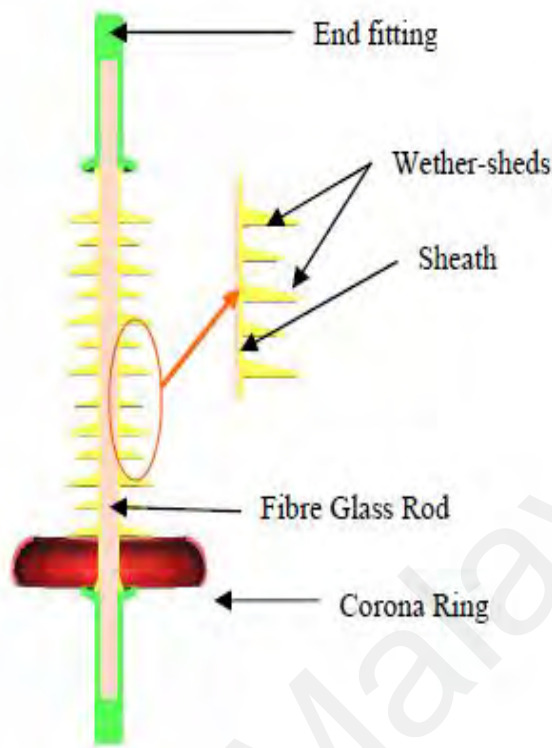
Figure 2.1: Components of a high voltage insulator string (Eleperuma, Saha, & Gillespie, 2008)

Non-ceramic insulators are also known as composite insulators. In earlier days, a replacement for porcelain and glass is non-ceramic insulators without a doubt in certain applications. However, many issues were encountered concerning their performance in the service, especially outdoor insulators that are exposed to environmental factors such as pollutions and ageing factors. Tracking and erosion of polymer sheds, chalking and crazing of sheds are the issues occur from the environmental factors. These factors may lead to higher contamination collection, arcing and flashover, electrical breakdown along the rod-shed interface and corona splitting of sheds. Outdoor insulators are at most risk to external flashover under contaminated conditions. This flashover experience along the insulators are impacted by few other elements such as humidity, ambient temperature and pollution of air (Arumugam, Haba, Koerner, Uhrlandt, & Paschen, 2018; Farzaneh & Chisholm, 2009). Air

pollution and moist conditions along the insulators are responsible for outdoor insulators flashover (Zheng, Wang, & Liu, 1993).

The main advantage of using polymeric insulator is its low surface energy and thereby, it can maintain good hydrophobic surface property in the wet conditions. The light weight of the composite insulators also an advantage to prevent the need to use heavy cranes for their installation and handling and this minimise the cost and also it is easy to install (Gubanski, 2005). The non-ceramic insulators have better performance in outdoor service in the presence of heavy pollution compared to ceramic insulators.

Non-ceramic insulators also have disadvantages in their performance. The main disadvantages are; non-ceramic insulators are depend on changes of chemical along the surface of insulator due to the environment and dry band arcing. Also, it is difficult to detect the fault in insulator and to evaluate its life expectancy. Polymeric insulators also suffer from erosion and tracking, which may lead ultimately to the failure of the insulator.

The obvious usage of non-ceramic composite insulators in many applications is mainly because of their advantages compared to the other insulators such as ceramic and glass insulator. However, the lifetime of non-ceramic insulators and their longer period of reliability are not popular since polymeric insulators are relatively new. Non-ceramic insulators might suffer from erosion and tracking and it could lead to the development of dry band arcing, which results to failure of polymeric insulators. Thus, it is important to understand weather factors and how they affect the materials in order to select a proper material.

The general requirements for an insulator are it should stand firm against the conductor tension, the reversible wind load as high as the frequency vibrations due to wind. The suspension and strain type of load are suitable with insulator. The diameter of composite insulator should be less than 200 mm (Taherian, 2019).

2.2.1 Structure of non-ceramic insulators

The basic construction of a polymer insulator for overhead line applications consists of a core, weather sheds and metal fittings are shown in Figure 2.2. Each component needs to be designed and optimised in order to get a satisfactory outcome in increasing the lifespan of non-ceramic insulators and electrical and mechanical performance.
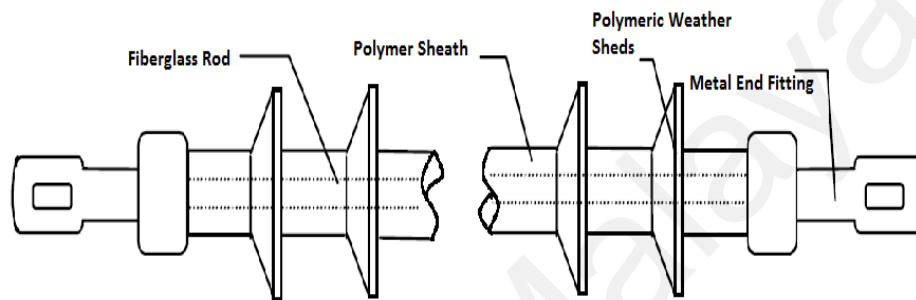
Figure 2.2: Simplified structure of non-ceramic insulators ("IEEE Guide for Application of Composite Insulators," 2002)

Figure 2.2 shows a simplified structure of a non-ceramic insulator. At the middle of the insulator is a fiberglass reinforced polymer (FRP) rod to distribute the tensile load (Kumar & Kalaivani, 2014; Mohammad, Hoseini, Mahdi, & Tavakoli, 2013). The center part of a non-ceramic insulator plays double burden. First is the insulating part and second is the load-bearing member, in suspension, cantilever or compression modes. The FRP rod is reinforced with few elements such as polyester, vinyl ester or epoxy resin to give proper mechanical strength (Chao & Huang, 2019; V, A. G, & U, 2021). Epoxy resin offers better electrical properties than polyester resins, which are applied in some cases to reduce the cost. Glass fibers are made of alkali-borosilicate glasses (E-glass), which are low alkali, lime-alumina borosilicate glass and showing acid corrosion due to high electrical integrity

and high resistance. The FRP rod shall be manufactured through pultrusion process. To avoid brittle fracture, chemical resistant alkali-aluminosilicate glass fibers should be used, also known as electrical corrosion resistant (ECR), which are able to withstand acid attacks. The FRP rod shall be void free. The main factor for the non-ceramic composite insulator design is the end seal. These seals are built by molding the sleeved core material into the end fitting and it is better due to the good physical bond obtained during molding.

Weather sheds are usually made from different type of insulator materials for electrical applications. The material used in composite weather sheds is the silicone elastomeric which bonded firmly to the sheath, vulcanised to the sheath and free from imperfections. The characteristics of silicone elastomers materials have shown success in outdoor electrical insulation applications with silicone elastomer meeting all the requirements for long-term performance. The materials over the rod are shaped and spaced in different methods to prevent the rod and it could lead to give highest electrical insulation between the end fittings (Eleperuma et al., 2008).

The sheath is the outer part of the core which prevents it from the environment. The sheath can be equipped together with weather sheds. The non-ceramic insulators engage a sheath made of insulating material and attach between the weather sheds and the core. Finally, mechanical load can be transmitted to core by end fittings. They are made of spheroidal graphite cast iron or forged steel. End fittings are connected to the rod by means of a controlled compression technique. Surrounding of the insulator is air having relative dielectric constant is energised on the lower end electrode while the upper end electrode connected with ground. Two dimensions of the two type composite insulators for finite element analysis are shown in Figure 2.3.
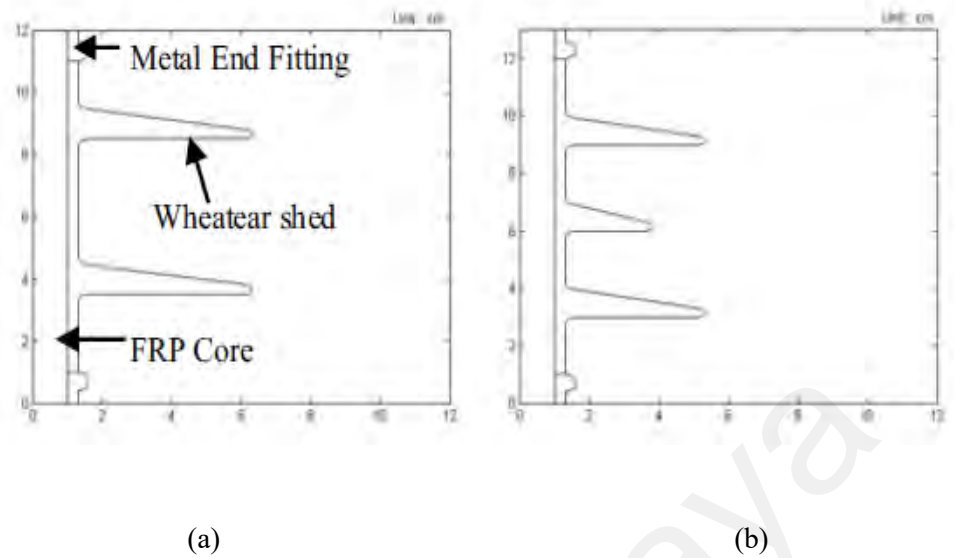
Figure 2.3: Two types of composite insulators for FEA; (a) Straight sheds and (b) Alternated sheds (W. Onchantuek & Oonsivilai, 2009)

There are mainly three types of insulators used in transmission lines system, which are the suspension/dead-end, line post insulators and guy strain. The design of hardware and the core size are the only differences among these three types. Several factors determine the number of units of an insulator string such as operation voltage, mechanical strength, sea level, lightning strength and contamination level of the environment (Hall, 1993). The capacity of insulator strings to withstand the voltage level when exposed is dependent on conditions such as the number of defective units, their position in the string and the position of the worker (Subcommittee, 2002).

Capacitances and stray capacitances are placed along the insulator string with the high voltage conductor and earth. Usually, capacitances are located between steel cap, pin and disc ceramic porcelain insulator. Figure 2.4 shows the primitive circuit of seven disc suspension insulator. Stray capacitance generally varies with the space and diameter of steel cap/pin of the insulator string and steel tower structure (Tonmitr, Tonmitr, & Kaneko, 2016).
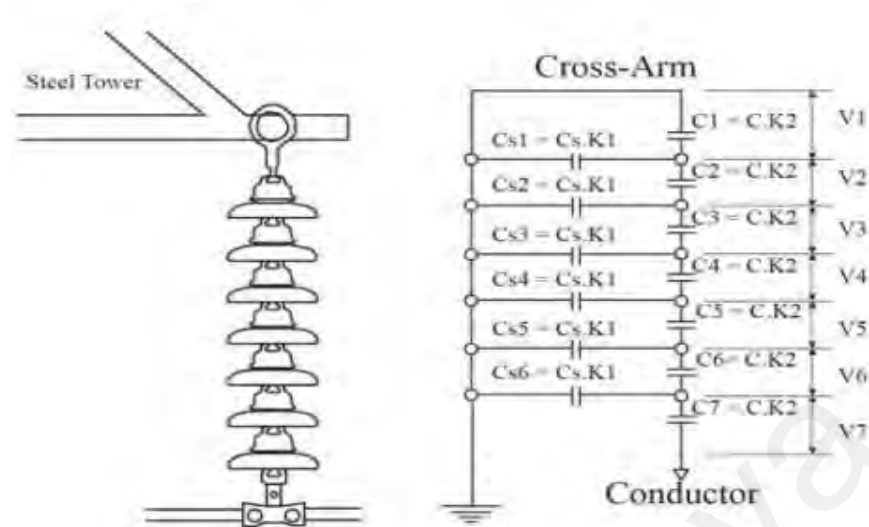
Figure 2.4: Simplified primitive circuit of seven disc along insulator (Tonmitr et al., 2016)

The distribution of voltage along the insulators is uneven because these capacitances have different values with different positions of each insulation disk (Ilhan & Ozdemir, 2007). Insulator disks nearer to the conductor are more highly stressed and have more uneven voltage distribution.

In general, the distribution of electric field magnitudes are higher near energised ends than grounded ends of a composite insulator (Phillips et al., 2008; Ross, 1987). Usually, the energised end is exposed to the highest electric field magnitudes. The position of the highest electric field occurs adjacent to the end fittings (Phillips et al., 2008; B. Vancia, Saha, & Gillespie, 2005). The distribution of electric field on the insulator surface is mainly affected by the capacitance and geometry of the insulator string. This is due to the lack of capacitor grading because a non-ceramic insulator is originated of one dielectric material between the energised and grounded ends. For non-ceramic insulators, the electric field should not exceed 4.5 kV/cm along the sheath for the dry uncontaminated composite

insulator and 3.5 kV/cm on the end fittings (M'Hamdi, Benmahamed, Teguar, Taha, & Ghoneim, 2022).

2.3   Corona Ring

Corona ring, also known as arcing ring is made of metal. Usually, corona ring is attached around the two ends of the insulator. Sometimes, the corona ring is placed around the energised end only if the voltage levels are below 345 kV (Murawwi & El-Hag, 2011). Corona rings are an opened torus i.e. circular geometry revolved about a center, made of conductive material, normally aluminum. Basically, aluminum is a lightweight material with high levels of corrosion resistance. The outer torus can be fully enclosed or have an opening (C-shaped) as shown in Figure 2.5 (Niedospial, 2012).

Opened Ring

Enclosed Ring

Figure 2.5: Typical Corona Rings (Niedospial, 2012)

The most important point in designing a corona ring is the geometry of the ring and its position. The important parameters are the diameter of the ring R, the tube radius r and the position of the ring H. One approach for designing the corona ring is by keeping two variables constant and changing the third variable (Murawwi & El-Hag, 2011). According to Illias et at, all these parameters have an impact on the electric field distribution along the

15

insulator string. The impact of the corona ring dimensions along the insulator of a 33 kV was analysed in (H. A. Illias et al., 2021). Corona tube settings determine the electric field strength of the insulator. The highest electric field is along the outer radius of the corona ring while the lowest electric field is at the inner radius of corona ring (Suat Ilhan, 2007). Whether raceway ring is opening or closed, it has small influence on the electric field and the arc of the raceway ring and two sides' circular rings. Based on Suat Ilhan et. al findings, the electric field strength at the raceway ring opening ball is larger than that at the same position of closed ring (Suat Ilhan, 2007).

There are many ways to have a better performance along the insulator by using corona rings. They are able to reduce few phenomenon such as corona discharge, the associated audible noise, radio interference and television interference (Wenxia Sima, Kun Wu, Qing Yang, & Caixin Sun, 2006). The job of the corona ring is to distribute the electric field gradient and reduce its maximum values below the corona threshold and protecting from corona discharge.

It is well known that the distributions of electric field and potential are influenced by many factors such as the transmission tower, magnitude of voltage, corona ring, and other environmental conditions. Corona rings are installed in order to achieve the optimal conditions where the potential voltage would be equally distributed along the insulators string (hamdi, Teguar, & Mekhaldi, 2013; Zhao & Comber, 2000). Commonly, corona rings are effective in improving the electric field voltage distribution (EFVD) along composite insulators, as well as in arc initiating and corona elimination (Gui-qing, 2009). Unluckily, there is no particular standard for the design and location of corona rings. Every manufacturer has their own recommendations for the installation of corona rings (Nicolopoulou, Gralista, Kontargyri, Gonos, & Stathopulos, 2011). Corona rings are

designed based on applied voltage of insulators and they are not interchangeable (Sebestyn, 2002).

When the corona rings have different voltage distribution, it may able to minimise the highest electric field at the energised end of the insulators. Corona ring able to remove the corona degradation of insulator materials. However, the correct ring must be used for the correct purpose to get the full benefits (Niedospial, 2012). Figure 2.6 and Figure 2.7 show the three different dimensions of corona ring.

The height of corona ring has a significant influence on the distribution of electric field. The optimum height of a corona ring along the high voltage insulator string will vary based on insulator applied voltage and it is influenced by the geometry of the end-fitting. The ring diameter also has an impact on the field, although not as significant as the ring height. The shape of the ring section makes a difference to the field at the live end and also on the field of the ring surface (Phillips, Childs, & Schneider, 1999; B. Vancia et al., 2005).
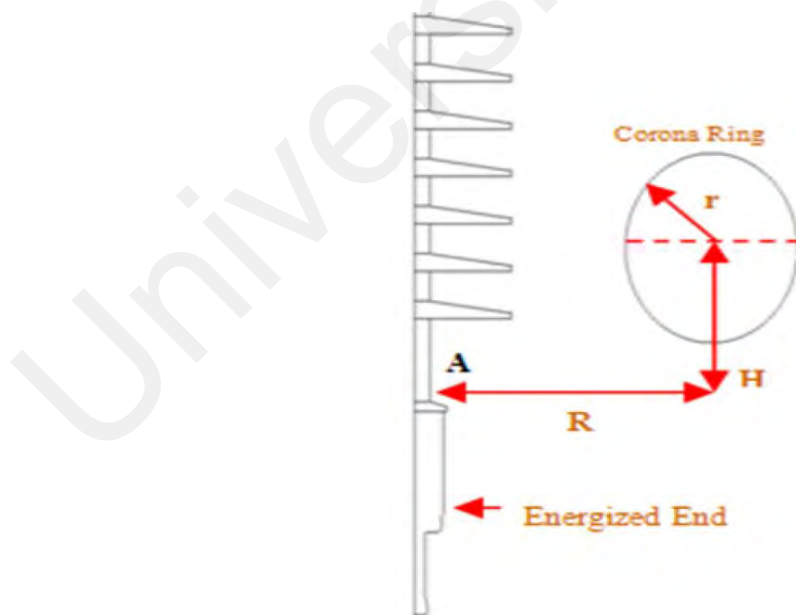
Figure 2.6: 2-D model of corona ring around energised end (Murawwi & El-Hag, 2011)

17
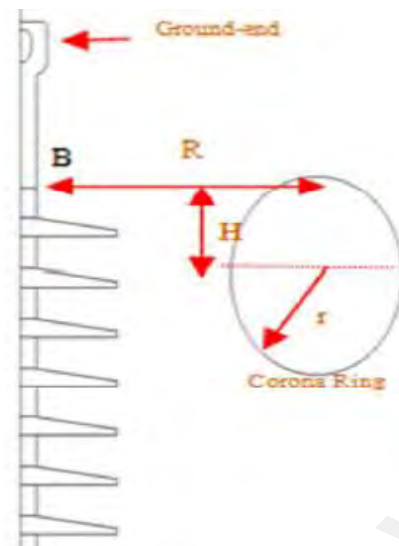
Figure 2.7: 2-D model of corona ring around ground end (Murawwi & El-Hag, 2011)

In the previous research works, neural network was engaged to deal with the optimisation of corona ring on composite insulators. To solve the long computing time problem of exhaustive method an optimisation of neural network model was established. Then, optimal scheme was obtained from the structure parameters of composite insulators. After the optimisation, the results show the lower surface field strength of the corona ring and the insulator field strength along the surface compared to the corona initial field strength (Qi-ying & Yong-sheng, 2011).

There are few critical characteristics to be considered when selecting a corona ring. Some of the characteristics are dry arc, leakage voltage, mechanical strength of insulator, type of attachment, mating feature, hot stick-able design, ordering and packaging. The size, shape and positioning along the insulator (height) of the corona rings vary from one manufacturer to another (B. Vancia, Saha, T.K. and Gillespie, T, 2001). Basically, the corona ring is installed at first or second shed of insulator string and there is no permanent standard to specify the dimension of grading ring required for a particular voltage level.

The size of the corona ring is proportional to the applied voltage of the system. The higher the voltage, the larger the corona rings need to be to successfully grade the electric field (Niedospial, 2012). No protection will be provided if the ring is in small size. The common corona ring diameters ∅, are shown in Table 2.1.

Table 2.1: Common corona ring diameters by voltage (Niedospial, 2012)

Line Voltages	≤230 kV		345 kV		500 kV	
	Line	Tower	Line	Tower	Line	Tower
∅	8-10"	none	11-13"	8"	15-17"	8-10"

For voltage ratings of 230 kV or below, the installation of corona rings are open to the recommendation by the manufacturer according to the requirements and installation (Dominguez, Espino-Cortes, & Gomez, 2013). The use of corona rings minimises the dry arcing distance of insulators, thereby increasing the length of the insulator. It can also be used to depress potential gradings along composite insulators and around the end fittings. With corona rings installed, the maximum stress of electric field area is transferred from the sections between the end fittings and the first shed to the outer side of the ring. Also, the maximum electric field can be reduced (Gui-qing, 2009).

The aim of the corona ring optimisation is to design an optimal dimension of corona ring when the maximum electric field along the insulator surface and corona ring surface are can be controlled below 4.5 kV/cm (the corona inception electric field strength of the insulator) (He & Gorur, 2014). The inclusion of corona ring along the insulator string will significantly minimise the percentage of voltage on the lowest part of insulators and will slowly increase the voltage sharing on the upper part of insulators. Hence, the distribution of potential will be more uniform by installing corona ring (Suat Ilhan, 2007).

2.4   Electric Field and Voltage Distribution

In order to achieve high electrical performance in high voltage networks, high voltage insulators are required. The insulator strings must have the capability to withstand the stresses from both electrical and mechanical (Eleperuma et al., 2008). The insulator types that are available in current market are ceramic insulators such as porcelain, glass insulator and non-ceramic such as polymer.

Basically, the electric field control is important especially in the main zones such as non-ceramic weather-shed surface, the interior of the fiberglass rod and the surfaces of metal fittings. The electric field and voltage distributions of insulator string are not uniform under applied voltage. The distribution of electric field along the insulator surface is not only depends on the applied voltage level but also on the insulator profile and the corona ring parameters (M'Hamdi et al., 2022; Moreno & Gorur, 1999). Because of the higher tower and longer insulator strings on UHV DC transmission line, the voltage distribution on insulator strings is more uneven compared to shorter insulator strings (Deng, Li, Zhang, Su, & Fan, 2009). The sheds near the energised end will experience maximum electric magnitude distribution due to the effect of the tower, shielding wire and transmission line. (Sima, Espino-Cortes, Cherney, & Jayaram, 2004). It also can cause corona discharge, surface deterioration of insulator and flashover. Hence, to reduce these effects, the calculation for electric field and voltage distribution is the essential way (Daochun, 2013). This is important where the energised end of a composite insulator is experienced to the maximum field magnitudes compared to the grounded ends of an insulator.

Typically, observation for peak magnitude can be done at the earthed end. The magnitude of electric field and potential along the insulators near conductors are higher compared to the insulators without corona ring (Akbari, Mirzaie, Rahimnejad, & Asadpoor, 2012). As in previous work, the control value of the electric field strength along the surface

of the grading and connectors are proposed according to the ANSI, CEA, ICE standards and IEEE guidelines (Wan et al., 2020).

Distribution of electric field can be calculated by using numerical simulation (Schümann, Barcikowski, Schreiber, Kärner, & Seifert, 2002). Figure 2.8 shows a shaded plot of electric field magnitude distribution on the polymer weather-shed surface of a suspension composite insulator as well as lines of equal potential surrounding the unit.
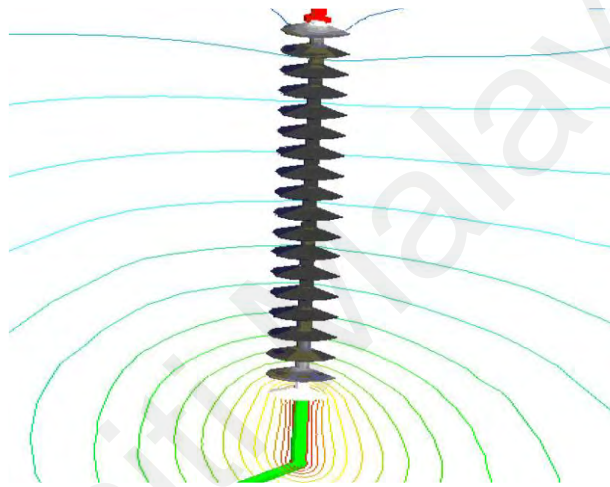
Figure 2.8: The electric field magnitude is indicated in grayscale with white being the highest and black the lowest ("Electric fields on AC composite transmission line insulators," 2008)

Facts and statistics collected from numerical method can be verified using a high voltage capacitive electric field probe.(Schümann, Barcikowski, Schreiber, C. Kärner, & M. Seifert, 2002). The usage of corona ring in industry has changed significantly, the results on surfaces of polymer housing (water drop corona) is because of physical discharge and electro-hydrodynamic (Phillips et al., 1999). To verify electrical surface field stresses by means of field calculation methods were suggested by (Weida, Steinmetz, & Clemens, 2008). Development of insulator string design and corona ring design are now suggested even at 115/123 kV compared to 161/170 kV in the past.

In the previous work, different techniques to mitigate the high electric field, ranging from the use of conventional corona rings to the use of composite polymeric materials were studied. They also suggested these techniques can be done with increasing the permittivity or electric field dependent conductivity (Cherney, 2005; Weida et al., 2008). Existing works have proposed the elimination of the first watershed and the modification of the shape next to the energised end to reduce the electric field (Araya, Montaña, & Schurch, 2021; Domínguez, Espino-Cortés, & Gómez, 2011).

The electric field distribution on the surface of insulators is a function of numerous parameters including applied voltage, insulator design, tower configuration, and corona ring and hardware design ("Electric fields on AC composite transmission line insulators," 2008). The uniformly distributed electric field along a polluted silicone rubber insulator string for AC applied voltage has been investigated in (Arshad, Nekahi, McMeekin, & Farzaneh, 2015; W. Onchantuek & Oonsivilai, 2009).
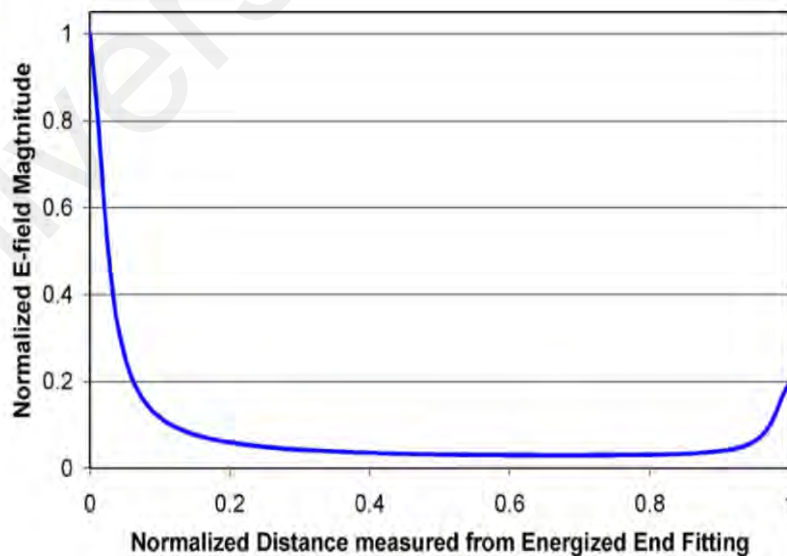
Figure 2.9: Plot of the normalised electric field ("Electric fields on AC composite transmission line insulators," 2008)

Figure 2.9 shows the normalised electric field magnitude within the fiberglass rod measured along an axial line. The electric field magnitude is high at the energised end and decreases exponentially along the insulator length. The magnitude increases again at the grounded end but to a far lesser extent. Few factors are affected the distribution of electric field along the insulator. The main factor is geometry of the insulator including the weather-shed system. Fiberglass rod, end settings and the electrical properties of polymer weather shed will affect the electric field magnitude. Other factors are the dimensions and position of the rings and their attachment method. Finally, the value of the energised line voltage is also one of the factors that influences the distribution of the electric field (Phillips et al., 2008). The presence of water droplets from rain and fog conditions causes the electric field enhancement. Discharges usually occur between water droplets and destroy the hydrophobicity of the polymer material surface (Weiguo Que, 2001).

In the previous works, a 33 kV of polymeric insulator was used for the simulations and distributions of electric field at both AC and DC were calculated. This could analyse the influence of type of voltage and the polarity for electric field and potential distribution (Arshad et al., 2015). Figure 2.10 shows 33 kV polymer insulators with pollution layer and Table 2.2 indicates the simulation parameters and insulator dimensions.
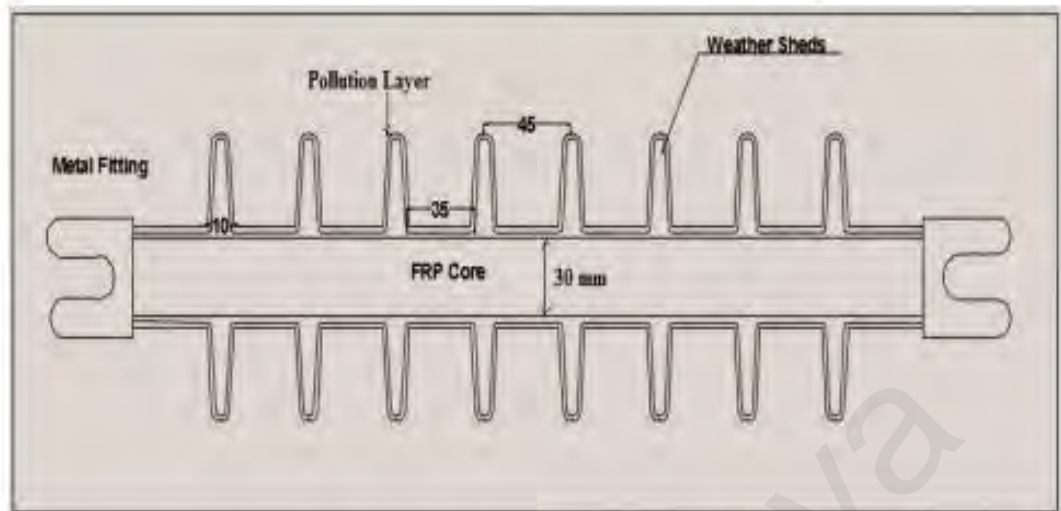
Figure 2.10: A 33 kV polymer insulator (Arshad et al., 2015)

Table 2.2: Simulation parameter and insulator dimensions (Arshad et al., 2015)

Number of sheds	8
Leakage Distance (mm)	900
Shed diameter (mm)	105
Sheath Diameter (mm)	30
Service voltage (kV)	33
Relative permittivity of SIR	4.3
Relative permittivity of FRP	7.2
Relative permittivity of water	81
Conductivity of pollution layer (μS/cm)	500
Conductivity of SIR (S/m)	1e-12
Conductivity of FRP (S/m)	0.004

2.5   COMSOL Multiphysics Software

The electric field evaluation is very complicated that an analytical method is quite hard to compute the accurate solutions. Numerical methods are thus assumed to derive proper solutions. Charge Simulation Method (CSM) method is used to determine the potential and

electric field values along insulator string (Shan, 1997). However, they simplify the problem without considering the influence of conductors and towers (Rashedi, Nezamabadi-pour, & Saryazdi, 2011).

A Finite Different Method (FDM) is used to determine the electric field in and around the insulators which is polluted with asymmetric boundary conditions. Another method that can be applied is Boundary Element Method (BEM), which is used to calculate the distribution of electric field and potential on insulator strings. This method considers the influences of conductors, grading devices and transmission line towers but computational method requirements were high (Rahimnejad & Mirzaie, 2012). Finite element analysis is a numerical technique for finding approximate solutions to boundary value problems for differential equations (Niedospial, 2012). It uses variation methods to minimise an error function and produce a stable solution.

COMSOL is a finite element method (FEM) software, solver and simulation software used for various physics and engineering simulation such as thermal field, acoustic, piezoelectric analysis. It allows the user to import *.MAT files, which can be used for simulation purposes or design the object in COMSOL. Material changes, building initial values, modifying designs and comparative study of the insulator properties can be done using this software (Sahu, Sahoo, & Karmakar, 2021).

2.6   Optimisation Techniques

In recent years, different types of algorithms are used by researchers in optimisation techniques. The behaviors of natural phenomena have encouraged researchers to apply in complex computational difficulties (Kim, Abraham, & Cho, 2007). The available complex computational difficulties are objective functions, control objectives, pattern recognition, image processing and filter modeling. At the same time, researchers have developed many

optimisation methods, such as Generic Algorithm, Simulated Annealing, Ant Colony Search Algorithm and Particle Swarm Optimisation. Different kinds of optimisation problems can be solved by these algorithms, depending on the type of problems since there is no specific algorithm suitable for all kinds of problems (Esmat Rashedi, Hossein Nezamabadi-pour , & Saryazdi, 2009).

In this research work, three different types of algorithms were used in order to obtain the lowest electric field magnitude along insulator models. These selected optimisation techniques are suitable in this work for their best solution in computational problems and various non-linear functions. Also, speed up the convergence and enhance the strength of optimisation.

2.7 Summary of the Chapter

In this chapter, overview of the insulator string and the electric field distributions is included. Minimising the electric field along the insulator has been studied by many researchers to improve the performance of insulator. Applications of the corona ring over the insulator string have also been discussed. A better understanding of installing corona ring along the insulator can be achieved through modelling. Apart of that, background of COMSOL Multiphysics software is explained.

A better understanding of electric field distributions along insulator string can be achieved through modelling that have been used by previous researchers that have been summarized in Table 2.3. The design of corona ring has been studied to minimise distributions of electric field and there are few methods that researchers have used is shown in Table 2.4.

Table 2.3: Model of insulator string

No.	Insulator string model	Proposed by	Year
1	380 kV V-insulator model	Suat Ilhan	2011
2	Polymeric insulator model	Arshad	2015
3	AC Composite insulator model	IEEE Taskforce	2008
4	3D E-field calculation model	Wenxia Sima, Kun Wu, Qing Yang, Caixin Sun	2006
5	Polluted surface insulator model	S. Muthu Kumar	2015
6	Silicone rubber insulator model	Esam Al Murrawi	2011

Table 2.4: Electric field measuring techniques

No.	Technique	Researcher	Year
1	Numerical simulations method	Arshad, A. Nekahi, S.G. McMeekin, M. Farzaneh	2015
2	3-D FEM method	R. Anbarasan and S. Usa	2015
3	OPERA simulations method	V.T. Kotargyi, L.N. Plati, I.F. Gonos, I.A. Stathopulos, A.M. Michaelides	2007
4	COMSOL Multiphysics method	Wenxia Sima, Kun Wu, Qing Yang, Caixin Sun	2006

CHAPTER 3: MODELLING OF INSULATOR STRING AND CORONA RING

3.1   Introduction

This chapter explains the methodology used in this work. The first step of the research is collecting information regarding the existing composite non-ceramic insulators. The design specifications and the details of material properties were gathered from articles, research papers and manufacturing company websites. The design of the insulator string and corona ring using finite element analysis (FEA) software are shown in this chapter. Important procedures and approaches were executed in order to achieve the desired results.

Two different insulator string models were used in this work. The development of a corona ring on 33 kV and 132 kV of insulator string model geometry is described in this section. The optimisation methods used in this work are also described, which are Gravitational Search Algorithm (GSA), Imperialist Competitive Algorithm (ICA) and Grey Wolf Optimisation (GWO). Optimisation involves the process of finding the best solution from all feasible solutions (Ramadhani, Hussain, Mokhlis, & Hajimolana, 2017). In the optimisation, the objective function is minimising the electric field magnitude around the energized ends of the insulator string while the ring diameter, the ring tube diameter and the vertical position of the ring along the insulator string are selected as the variables.

3.2   Design and simulation of non-ceramic insulator strings and corona ring model

COMSOL Multiphysics with MATLAB software was used in this project. A three-dimensional (3D) axial symmetric geometry and two-dimensional (2D) axial symmetric geometry of the insulator strings were modeled using this software. Both three-dimensional Finite Element Method (3D-FEM) and two-dimensional Finite Element Method (2D-FEM) are suitable tool since both symmetrical (mirror-or-rotational) and non-symmetrical

geometries can be considered in the field calculation (Stefanini, Seifert, Clemens, & Weida, 2010; Yang, Zhu, Tian, Zhu, & Yang, 2020). The specifications of the material were defined in the model. The mesh was built using mesh building option once the initial values are assigned. Then, the results were computed. In designing, the geometry was drawn according to the actual geometry of the insulator string.

Figure 3.1 shows three-dimensional (3D) model geometry of a 33 kV composite insulator and corona ring that has been developed in this work. The dimensions of the insulator string were drawn according to an insulator string available from the manufacturer. The top iron was connected to the ground while the bottom iron was supplied with a 33 kV applied voltage. The whole model was surrounded with air to compute the electric field magnitude on the insulator surface. The outer boundary for air was set to zero charge to build an infinite air region as a limited region (Bakar et al., 2016; Hazlee Azil Illias, Abd Halim, Abu Bakar, & Mokhlis, 2015). Table 3.1 shows the data of the insulator string used in this work, which has basic insulation level of 200 kV.
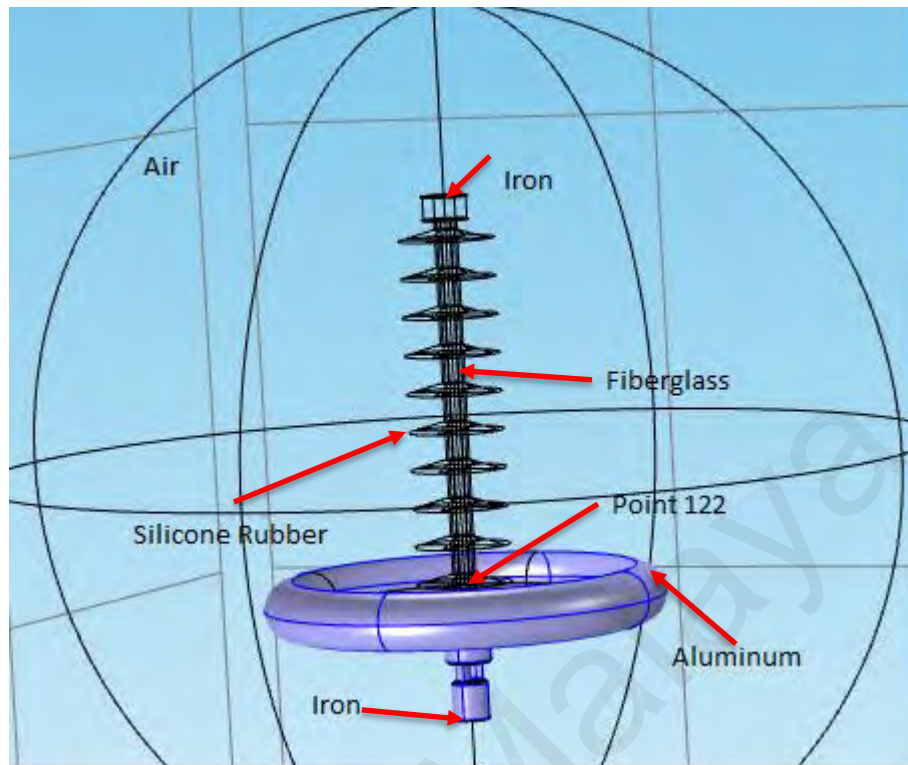
Figure 3.1: A 3D model geometry of composite insulator and corona ring

Table 3.1: Dimensions of insulator string for 33 kV system voltage (Insulator, 2013)

Typical System Voltage	No. of Sheds	Length (mm)	Cantilever Strength (kN)	Creepage distance (mm)
33 kV	10	458	10	950

Figure 3.2 shows two-dimensional (2D) model geometry of a 132 kV composite insulator and corona ring that has been developed in this work. Similar to 33 kV insulator, the dimensions of the insulator string were drawn according to an insulator string available from the manufacturer. The top iron was connected to the ground while the bottom iron was supplied with a 132 kV applied voltage. The whole model was surrounded with air to compute the electric field magnitude on the insulator surface. The outer air boundary was

set to zero charge to model an infinite air region as a limited region. Table 3.2 shows the data of the insulator string used in this work.
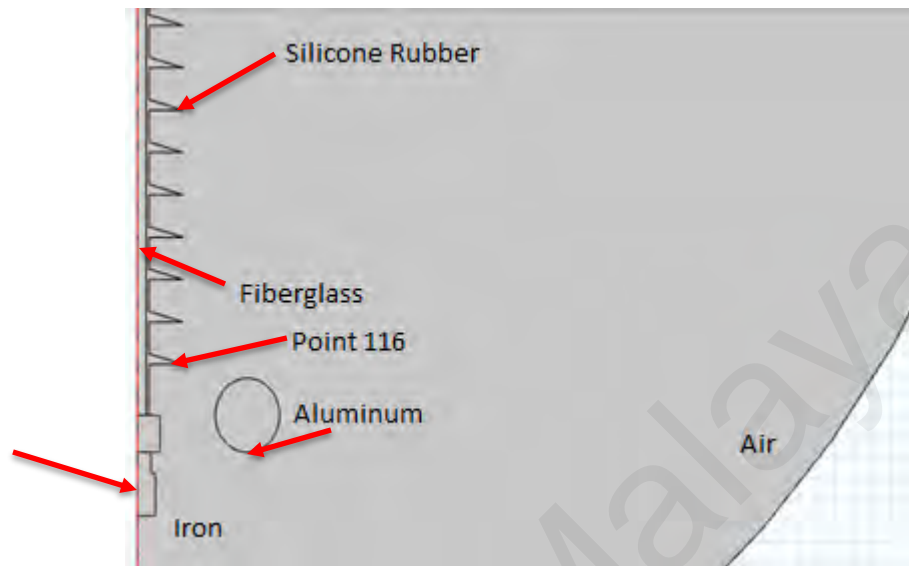
Figure 3.2: A 2D model geometry of composite insulator and corona ring

Table 3.2: Dimensions of insulator string for 132 kV system voltage (Liaoning Mec Group CO, 2012)

Typical System Voltage	No. of Sheds	Length (mm)	Cantilever Strength (kN)	Creepage distance (mm)
132 kV	40	1650	6.8	3914

Figure 3.3 shows a corona ring and its dimensions, which are the ring diameter (R), diameter of ring tube (r) and vertical position of the ring along the insulator (H). These dimensions were set as the variables for the optimisation algorithms in order to achieve the lowest electric field along the insulator string. The size of corona ring installed with insulator string has strong influence of electric field distributions. This corona ring and its dimensions are applied in both 33 kV and 132 kV.

31
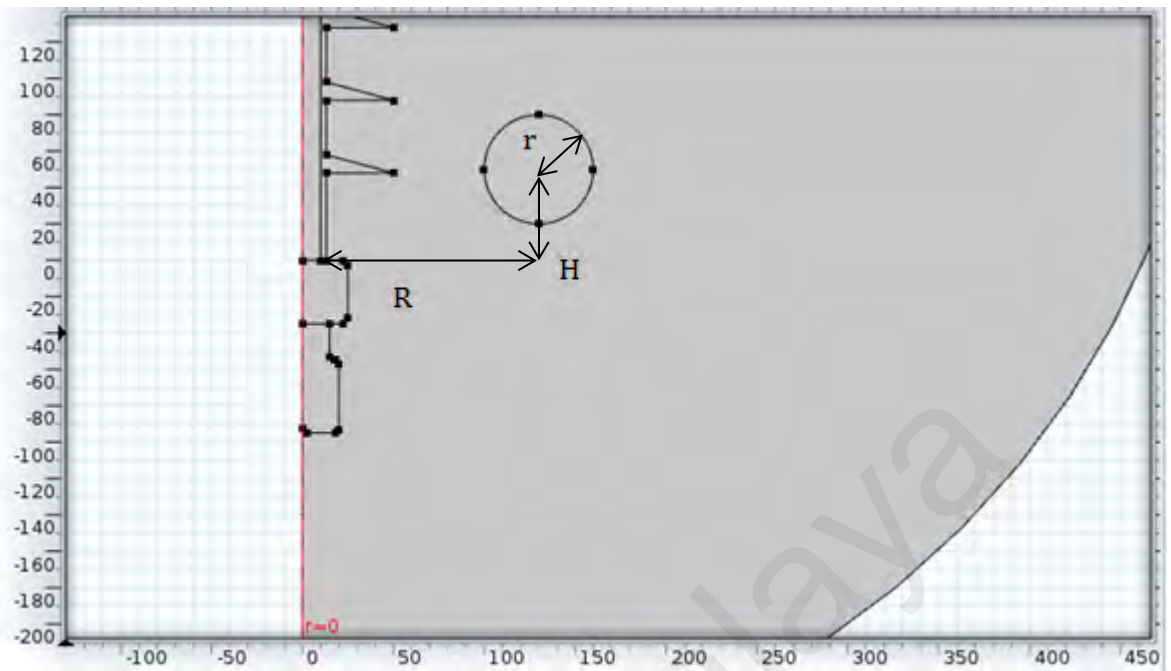
Figure 3.3: Dimensions of corona ring

3.2.1 Modeling of non-ceramic insulator

The insulator string is modeled based on the dimensions from the actual insulator string for 33 kV and 132 kV applied voltage. The total length of the insulator and its number of weather sheds are shown as in Table 3.1 and Table 3.2. A fiberglass rod located at the center of the insulator and an iron end fitting at both ground and energised ends. The insulator is made by silicone rubber and the whole geometry model was surrounded by air boundary.

3.2.2 Material and boundary settings

The relative permittivity ε_r and electrical conductivity σ of each material in the model were assigned as listed in Table 3.3. Table 3.4 shows the boundary conditions of the model were set with relevant interface settings. The boundary conditions for electric field analysis are available with the AC/DC Module, such as the capability to give the total

electric field on a boundary. The terminal of the insulator was applied at terminal with a voltage of 33 kV and 132 kV with presence of harmonic while the bottom of the insulator was grounded with 0 V. The outer part of the insulator was enclosed by a layer of air. All interiors were set to continuity.

Table 3.3: Properties of material for each part in the model

Property Materials	Relative Permittivity, ε_r	Electrical Conductivity, σ (S/m)	Density, ρ (kg/m³)	Heat Capacity at a constant pressure, C_p (J/kgK)	Thermal Conductivity, k (W/mK)
Aluminum	1	3.774×10^7	2700	900	160
Silicone Rubber	4.2	1×10^{-14}	2203	1925	1.38
Fiberglass	4.2	1×10^{-14}	80	390	0.47
Iron	1	1.12×10^7	7870	440	76.2
Air	1	0	1	450	0.024

Table 3.4: Boundary setting of the electric field

Boundary	Boundary condition
Terminal	Applied voltage 33 kV & 132 kV
Air	Electric insulation
Ground	0 V
All interior boundary	Continuity

3.2.3   Meshing

After the boundary and material were set, the model was meshed. By using the elementary shape functions, the model in FEA evaluates the solution of domain, boundary, edge and point of insulator string. The shape function can be constant, linear or higher order. A finer or coarser mesh is required to obtain an accurate result based on the element order in the insulator string model. The size of the elements used for air was normal and all

the domains of the model using finer element. Figure 3.4 and Figure 3.5 show the meshing

elements in the model.
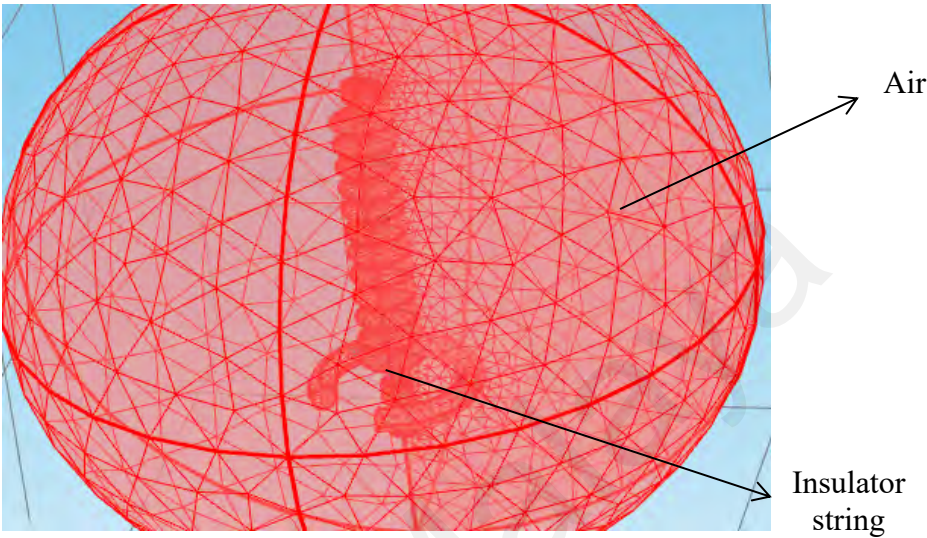
Figure 3.4: Meshing elements in 3D model
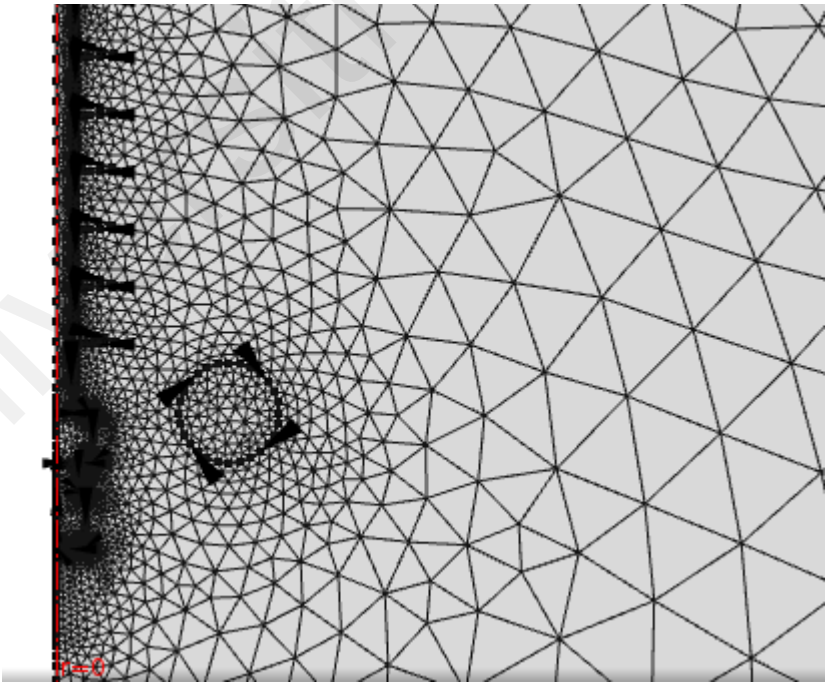
Figure 3.5: Meshing elements in 2D model

3.2.4 Electric field equations

The equations applied to obtain the electric potential distribution in the model is governed by (Bakar et al., 2016; Winai Onchantuek & Oonsivilai, 2008)

$$-\nabla . \varepsilon 0 \varepsilon r \, \nabla V \;=\; 0 \tag{3.1}$$

where ε_0 is the vacuum permittivity and ε_r is the relative permittivity of the material. The boundary condition between two dielectrics is

$$n . (D1 - D2) \;=\; 0 \tag{3.2}$$

where n is the unit vector normal to the surface and D_1 and D_2 are the electric displacement respectively.

The boundary condition of the high voltage terminal is

$$V = V_0 \tag{3.3}$$

where V_0 is the applied voltage. The ground boundary condition is (Hazlee Azil Illias et al., 2015)

$$V \;=\; 0 \tag{3.4}$$

3.3 Imperialist Competitive Algorithm (ICA)

ICA is a mathematical model and the computer simulation of human social evolution. It is also socio-political metaheuristics inspired by historical colonization process and competition among imperialist to capture more colonies. ICA is a new algorithm that was proposed by Esmaeil Atashpaz Gargari and Caro Lucas in 2007 (Atashpaz-Gargari & Lucas, 2007; Rout, Sahu, & Panda, 2013). ICA was used because it has considerable improvement over other nature-inspired algorithms in finding the optimum solution in less computational time with the same population size and iterations.

ICA is a socio-politically motivated optimisation algorithm, which is similar to many other evolutionary algorithms and starts with a random initial population or empires. The basic idea of evolutionary competition is initiated from the idea of natural choice or survival of the fittest defined by the famous naturalist Charles Darwin. Thus, optimisation is similar to the method of the preservation of favorable individual difference and variations and the destruction of those that are injurious (Zhang, Wang, & Peng, 2009). Three optimisation methods were used in the research including ICA and other two methods; ant colony optimisation (ACO) and particle swarm optimisation (PSO). These methods were used to optimise load sharing and the results show that it can reduce fuel consumption and the battery lifetime can be increased.

Even though ICA was introduced recently, it has been successful in a wide range of applications, such as adaptive antenna arrays, intelligent recommender systems, optimal controller for industrial and chemical possesses (Bashiri & Bagheri, 2012; Zhang et al., 2009). Imperialistic competition approaches to a condition in which there exists only one empire and its colonies are in the same position (Chen & Imani Marrani, 2020; Soroudi & Ehsan, 2012). Most of the researchers concluded that ICA is more effective in exploring the search space and produces more promising results. This makes ICA the best optimisation technique for long-term reconfiguration problems. References that have studied the ICA, altogether acknowledge the power of the ICA in optimising high-dimensional problems. Figure 3.6 shows the flowchart of ICA algorithm used in this work.

Initially, the countries were generated randomly as population (H. A. Illias, Mou, & Bakar, 2017; Soroudi & Ehsan, 2012). In this work, the dimension of the optimisation problem N_{var} is 3. A country is 1 x N_{var} array, defined as

$$Country = [r, R, H] \tag{3.5}$$

N_{imp} is selected from the stronger countries to create the empires. The remaining number of the population N_{col} will be the colonies. As a result, a country is divided into colonies and imperialists. A normalised cost of an imperialist is defined as

$$C_n = c_n - max\ (C_i) \tag{3.6}$$

where c_n is the cost of nth imperialist and C_n is its normalised cost. The normalised power of each imperialist is defined by

$$p_n = \left| \frac{C_n}{\sum_{i=1}^{Nimp} C_i} \right| \tag{3.7}$$

Thus, the starting number of colonies of an empire is

$$NoC_n = round\ (p_n\ N_{col}) \tag{3.8}$$

where NoC_n is the initial number of colonies of *n*-th empire.

Each colony from the population will move towards the imperialist by *x*-unit in the direction of the vector from colony to imperialist. *x*-unit is a random variable with uniform distribution. Hence,

$$x \sim U(0, \beta \times d), \beta > 1 \tag{3.9}$$

where d is the distance between the colony and imperialist. β causes the colony to become closer to the imperialist.

Some colonies are randomly selected and change their positions to allow for more freedom in the search space. The number of colonies in the empire, which is assumed to be replaced with the same number of newly generated countries, is

$$NRC = round\{RevolutionRate \times No.(The\ colonies\ of\ empire_n)\} \tag{3.10}$$

where *NRC* is the number of revolutionary colonies.

The total power of an empire depends on its own all colonies, given by

$$TC_n = cost(imperialist_n) + \xi \, mean(cost(colonies \; of \; empire_n)) \tag{3.11}$$

where ξ is a position coefficient.

Then, imperialist competition happens between all empires. The power of the weaker empires will start to reduce and the power of more powerful empire will increase. Hence, the possession probability of each empire is based on its total power. The normalised total cost is

$$NTC_n = TC_n - max\{TC_i\} \tag{3.12}$$

where TC_n and NTC_n are the total cost and the normalised total cost of n-th empire respectively. The possession probability of each empire is calculated by

$$P_{pn} = \left| \frac{NTC_n}{\sum_{i=1}^{Nimp} NTC_i} \right| \tag{3.13}$$

A vector P is formed as

$$P = [p_{p1}, p_{p2}, p_{p3}, \dots, p_{pNimp}] \tag{3.14}$$

A vector R with uniformly distributed elements is also formed as

$$R = [r_1, r_2, r_3, \dots, r_{Nimp}] \tag{3.15}$$

Thus, a vector D is given by

$$D = P - R = [D_1, D_2, D_3, \dots \dots D_{Nimp}] \tag{3.16}$$

The elements of D will hand the mentioned colonies to an empire whose relevant index in D is maximum. The empire will collapse and become one of the rest colonies when it loses all of its colonies (Nosratabadi et al., 2020; Shirkouhi, Eivazy, Ghodsi, Rezaie, & Atashpaz-Gargari, 2010). Finally, only the most powerful empire with no competitor will remain. Hence, all colonies will have the same costs with the unique empire (H. A. Illias et al., 2017; Rashtchi, Rahimpour, & Shahrouzi, 2012).
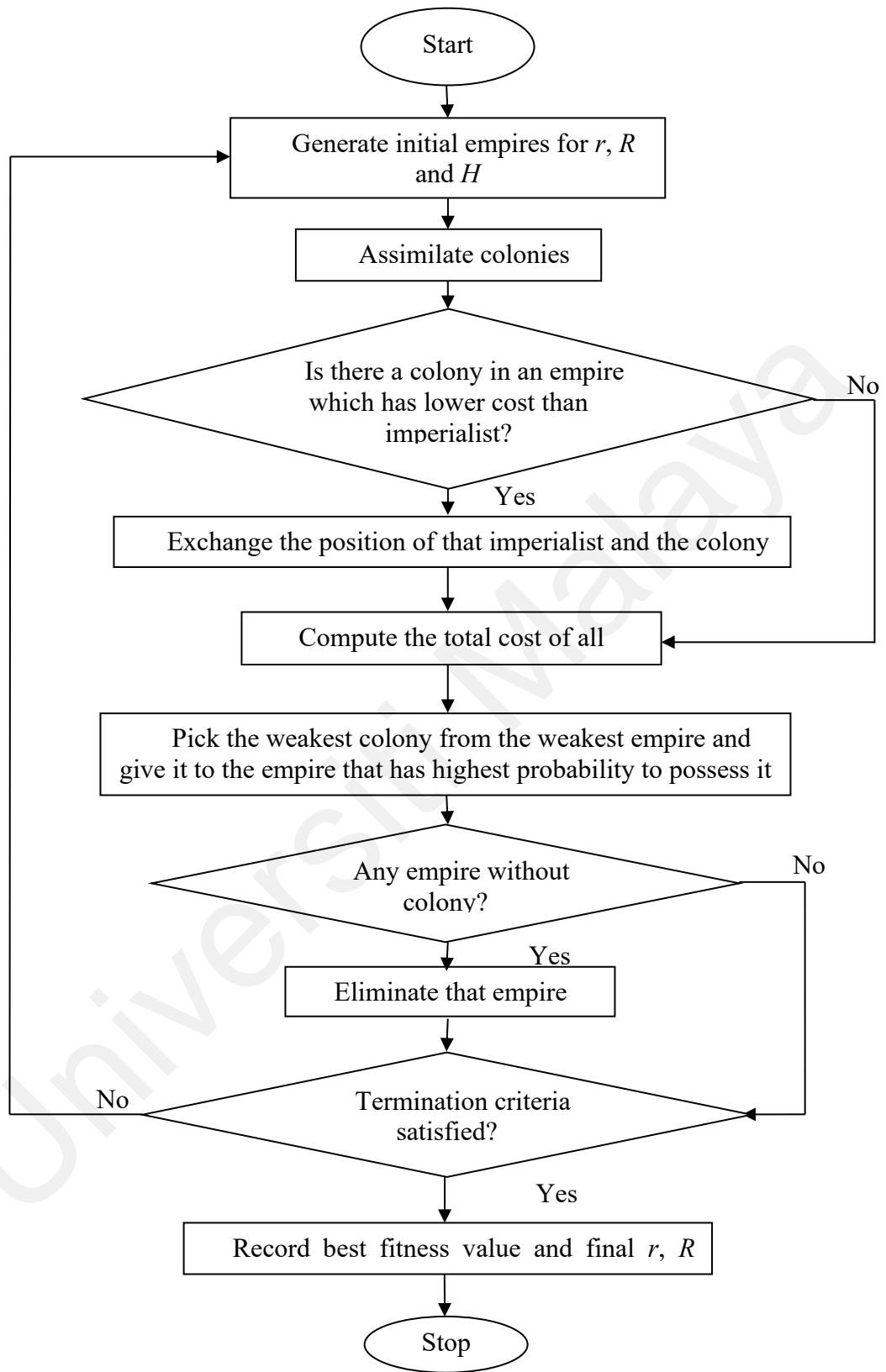
Figure 3.6: Flowchart of ICA algorithm used in this work

3.4   Gravitational Search Algorithm (GSA)

A simulation of human intelligence in machines that are programmed to operate like humans known as Artificial Intelligent (AI). Artificial Intelligent methods are a special class of heuristic search methods. Intelligent based optimisation methods have also been utilised in finding optimum dimensions (Ing, Mokhlis, Illias, Aman, & Jamian, 2015). One of the techniques is Gravitational search algorithm (GSA) which is based on Newton's law of gravitational forces and the law of motion (Rashedi et al., 2011; Sabri, Puteh, & Mahmood, 2013). The efficiency of Artificial Intelligent methods has become a matter of concern due to the high complexity of multi-objective problems (Hassanzadeh & Rouhani, 2010). GSA is well suited to solve computational problems. GSA has already been used in many problems such as economic dispatch, unit commitment optimal load flow, etc. In GSA, the final solution is taken as an object in the search space. Each object has different dimensions and positions, representing the variables (Puri, Chauhan, & Singh, 2015). Each object experiences a force of attraction towards object due to gravitational force between objects with different positions. These positions stop at one point as those are the optimal solution in the search space.

In GSA, the agents are taken into consideration as the objects and their masses are measured based on their performance. Every object represents a solution to the problem. The objects are attracting each other by the gravity force and this force causes a global movement of all objects. The heavier masses have higher fitness values; these fitness values present a good optimal solution to the problem and they move slower than lighter ones, which is representing worse solutions.

Esmat Rashedi also used GSA to present a new linear and nonlinear filter modeling. In the study, the author considered unknown filter parameters as a vector to be optimised.

In order to verify the efficiency of the proposed GSA-based filter modeling, genetic algorithm (GA) and particle swarm optimisation (PSO) were used to compare the obtained results (Rashedi et al., 2011).

Figure 3.7 shows the flowchart of GSA algorithm used in this work. At the starting of the algorithm, the position of a system is described with N masses according to

$$Mass_i = [r_i^1, R_i^2, H_i^3, P_i^4] \qquad \text{for } i = 1, 2, \dots N_{mass} \tag{3.17}$$

where N_{mass} is the number of masses in the population defined by the user. Then, the fitness of each mass is evaluated. A gravitational constant G is initialised at the starting of the operation and is reducing with iteration. The gravitational constant G is calculated by

$$G\ (iter) = G_0 \exp(-\alpha \frac{iter}{\max iter}) \tag{3.18}$$

where $iter$ is the current iteration, α is a user specified constant, G_0 is the initial value of gravitational constant and $maxiter$ is the total number of iterations.

Fitness evaluation is used to compute the masses of the agents. Heavier mass of an agent has more influence. The masses are updated by

$$M_{ai} = M_{pi} = M_{ii} = M_i$$

$$m_i(iter) = \frac{fit_i(iter) - worst\ (iter)}{best\ (iter) - worst\ (iter)} \tag{3.19}$$

$$M_i(iter) = \frac{m_i(iter)}{\sum_{j=1}^{Nmass} m_j(iter)} \tag{3.20}$$

where $fit_i(iter)$ is the fitness value of mass i at iteration $iter$ and $m_i(iter)$ is the mass of i at current iteration. For a minimisation problem, it is calculated by

$$best\ (iter) = min_{j \in \{1, \dots Nmass\}} fit_j(iter) \tag{3.21}$$

$$worst\ (iter) = min_{j \in \{1, \dots Nmass\}} fit_j(iter) \tag{3.22}$$

The next step is to calculate the total force in different directions. The gravitational force F_{ij} of i due to mass j at current iteration *iter* is calculated by

$$F_{ij}(iter) = G(iter)\frac{M_i(iter)}{R_{ij}(iter)^{Rpower}+\varepsilon}(Mass_j(iter) - Mass_i(iter)) \tag{3.23}$$

where M_i is the inertial mass of mass i, M_j is the inertial mass of mass j, ε is a constant, R_{ij} is the Euclidian distance between i and j masses and R_{power} is the power of Euclidian distance.

The total force $F_i^d(iter)$ that acts on agent i in a dimension d is a randomly weighted sum of *d-th* components from other agents. *rand$_j$* is a random number that falls between (H. A. Illias et al., 2017). $F_i^d(iter)$ is calculated using

$$F_i^d(iter) = \sum_{j \in kbest, j \neq i}^{N_{mass}} rand_j F_{ij}^d(iter) \tag{3.24}$$

The acceleration of the agent i at time t and in direction *d-th*, $a_i^d(iter)$ is given by

$$a_i^d(iter) = \frac{F_i^d(iter)}{M_{ii}(iter)} \tag{3.25}$$

The next position of a mass is updated by

$$Mass_i^d(iter + 1) = Mass_i^d(iter) + v_i^d(iter + 1) \tag{3.26}$$

where $v_i^d(iter + 1)$ is the next velocity of a mass given by

$$v_i^d(iter + 1) = rand_i v_i^d(iter) + a_i^d(iter) \tag{3.27}$$

Finally, the algorithm stops when the maximum number of iterations is attained (H. A. Illias et al., 2017).
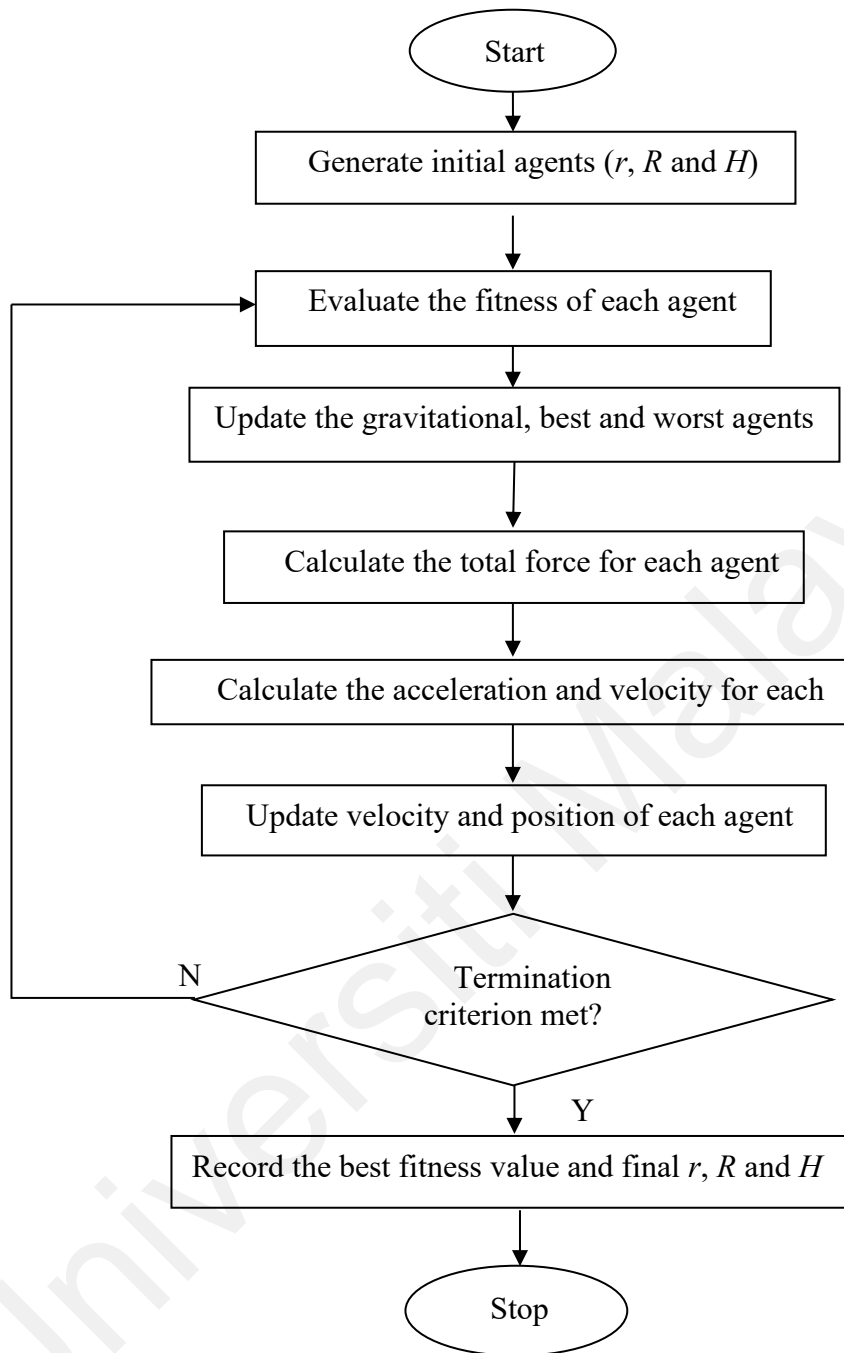
Figure 3.7: Flowchart of GSA algorithm used in this work

Start

Generate initial agents (r, R and H)

Evaluate the fitness of each agent

Update the gravitational, best and worst agents

Calculate the total force for each agent

Calculate the acceleration and velocity for each

Update velocity and position of each agent

Termination criterion met?

N

Y

Record the best fitness value and final r, R and H

Stop

3.5   Grey Wolf Optimisation (GWO)

Grey wolf optimisation (GWO) algorithm was proposed in 2014 by Mirjalili et al (Mirjalili, Mirjalili, & Lewis, 2014). GWO is a developed computational method in swarm intelligence algorithms, which replicates the grey wolves preying behavior. This algorithm has better results to settle the complicated engineering problems. For the purpose of speed up the convergence and enhance the strength of optimisation, various upgraded GWO algorithms have arised (Yan, Chen, & Ma, 2019). The advantages of using GWO are it improves the global search performance, speed up the convergence of the algorithms and global search capability dynamically compared to the other type of swarm intelligence algorithms (Raj & Bhattacharyya, 2018; Yu, Yu, Liu, Wang, & Gao, 2016). Convergence factor in the search space is balancing the capability of the algorithm for both global search and local search (Han & Tong, 2020).

To solve the optimisation problem in GWO, the behavior of grey for hunting is modeled (Dhavakumar & Gopalan, 2021; Naserbegi, Aghaie, & Zolfaghari, 2020). The social hierarchy of grey wolves consists of 4 groups. The leaders of the group are called alphas or dominant wolves. They are responsible for making decisions about resting spots, time to sleep or wake and hunting. Basically, the alphas motives are to give commands to the group. The second class is beta grey wolves. Betas are dependent wolves and support the alphas in leadership and purpose making. The main task of betas is to consult the alphas wolves (Dutta & Nayak, 2021; Naserbegi et al., 2020).

Omega is the third stage of grey wolves. The omega wolves are realised as a scapegoat. Omegas should give in to alphas and betas wolves. The whole set faces troubles if the omega wolves are lost. The fourth and last stage are the delta wolves. They were once either alpha or beta wolves. Delta must comply with alpha and beta, but they dominate omega. Alpha and beta have to help other group members whenever they are needed

(Mirjalili et al., 2014; Naserbegi et al., 2020). The steps of GWO algorithm are illustrated in Figure 3.8.
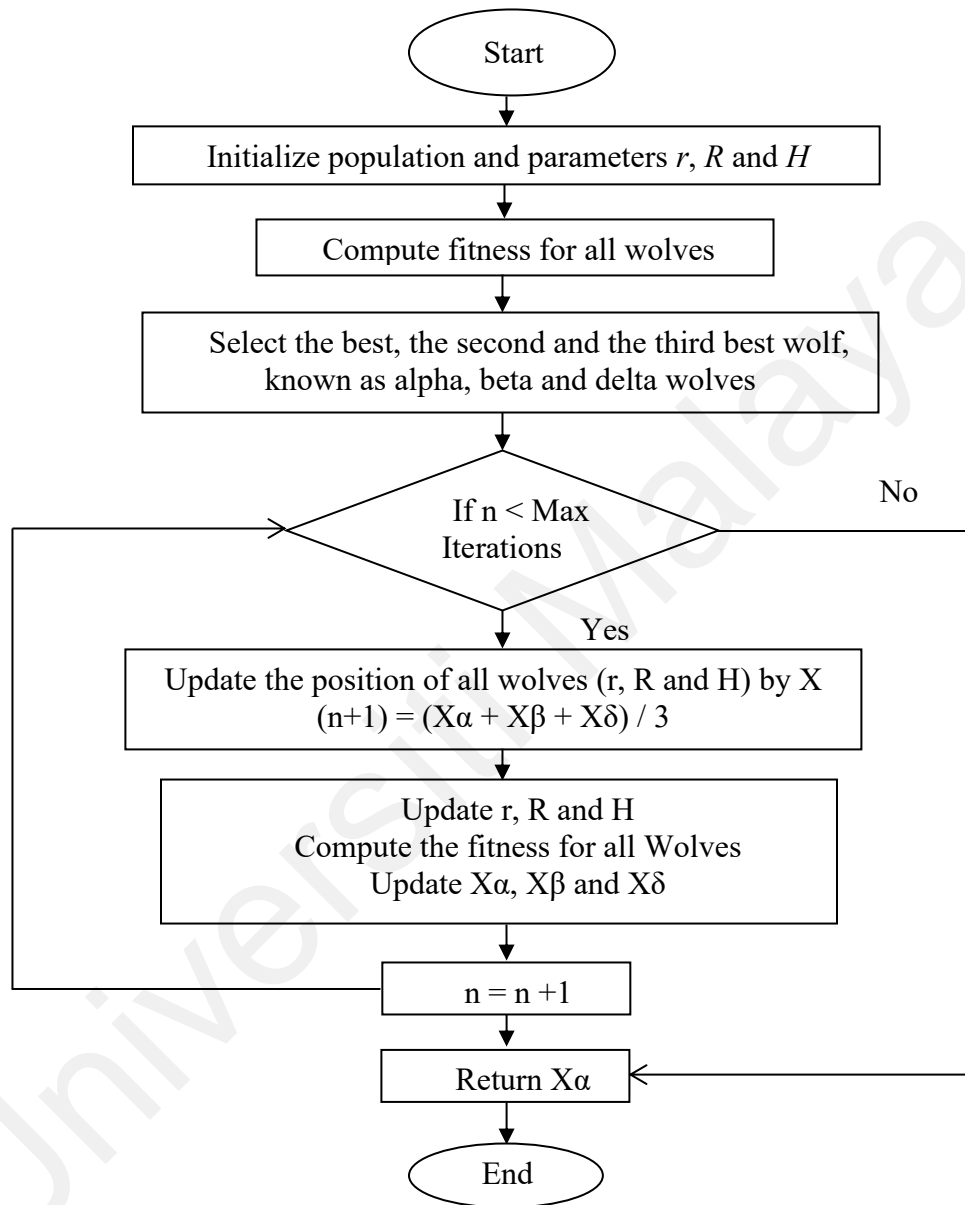
Figure 3.8: Flowchart of GWO algorithm used in this work

Generally, grey wolves surround the hunt while hunting and then approach the hunt until it ceases and in the end attacks it. In GWO, the best solution is considered as alpha, followed by beta, and omega and delta are given priority respectively (Miao, Chen, Zhao, & Demsas, 2020). If X_p is considered as the vector that shows the position of the prey, the grey wolves' position is identified by vectors as shown in equation (3.28) and (3.29),

$$\vec{X}(t+1) = \overrightarrow{X_p}(t) - \vec{A}.\vec{D} \tag{3.28}$$

$$\vec{D} = \left| \vec{C}.\overrightarrow{X_p}(t) - \vec{X}(t) \right| \tag{3.29}$$

From the equations above, t is iteration number, and $\vec{A}$ and $\vec{C}$ indicate factor vectors that computed according to equations (3.30) and (3.31),

$$\vec{A} = 2\vec{a}.\overrightarrow{r_1} - \vec{a} \tag{3.30}$$

$$\vec{C} = 2.\overrightarrow{r_2} \tag{3.31}$$

where the ingredients of $\vec{a}$ are linearly decrease from 2 to 0 over the iteration period. $\overrightarrow{r_1}$ and $\overrightarrow{r_2}$ are random vectors in [0, 1]. The wolves, alpha, beta and delta are recognized as the top three solutions. Omega and other wolves update their position as their best solutions. The above contents are presented with equations (3.32) to (3.38) (Miao et al., 2020).

$$\overrightarrow{D_\alpha} = \left| \overrightarrow{C_1}.\overrightarrow{X_\alpha} - \vec{X} \right| \tag{3.32}$$

$$\overrightarrow{D_\beta} = \left| \overrightarrow{C_2}.\overrightarrow{X_\beta} - \vec{X} \right| \tag{3.33}$$

$$\overrightarrow{D_\delta} = \left| \overrightarrow{C_3}.\overrightarrow{X_\delta} - \vec{X} \right| \tag{3.34}$$

$$\overrightarrow{X_1} = \overrightarrow{X_\alpha} - \overrightarrow{A_1}.\left(\overrightarrow{D_\alpha} \right) \tag{3.35}$$

$$\overrightarrow{X_2} = \overrightarrow{X_\beta} - \overrightarrow{A_2}.\left(\overrightarrow{D_\beta} \right) \tag{3.36}$$

$$\overrightarrow{X_3} = \overrightarrow{X_\delta} - \overrightarrow{A_3}.\left(\overrightarrow{D_\delta} \right) \tag{3.37}$$

$$\vec{X}(t+1) = \frac{\overrightarrow{X_1}+\overrightarrow{X_2}+\overrightarrow{X_3}}{3} \tag{3.38}$$

Figure 3.9 shows the steps for the search agent matching positions of alpha, beta and delta. All the three wolves evaluate the position of the hunt and then the other wolves update their position randomly close to the hunt. This procedure continues until the desired condition is met (Naserbegi et al., 2020).
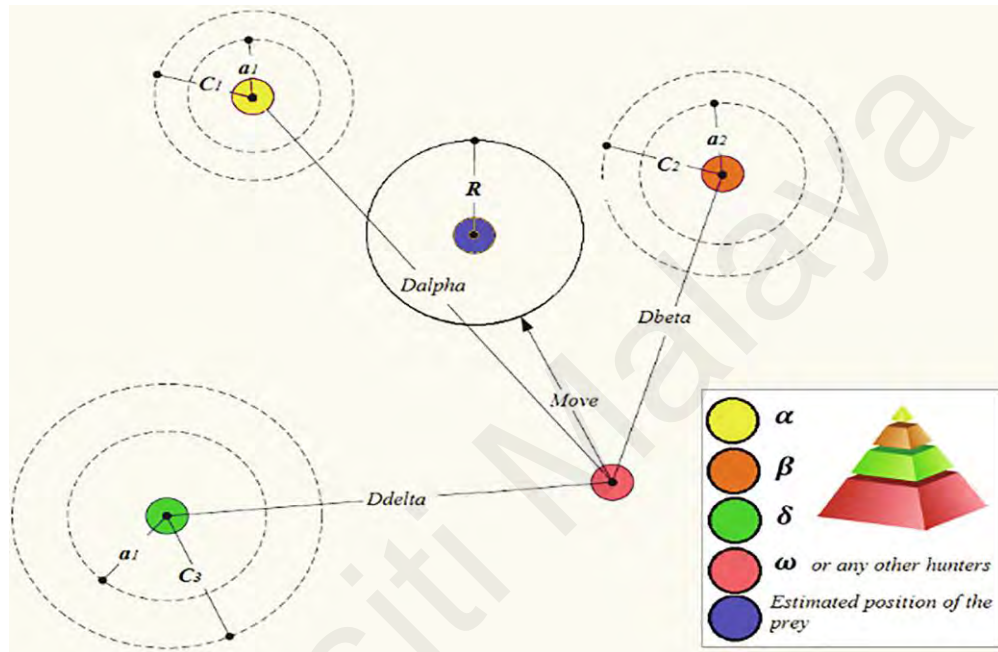
Figure 3.9: The update steps for grey wolves position (Naserbegi et al., 2020)

3.6   Summary of the Chapter

Models describing a 33 kV and 132 kV insulator string with corona ring are developed using Finite Element Analysis (FEA) method. The advantages of using this method over other methods are any shape of the geometry can be modeled easily, has the potential to generate electric field distribution and electric potential distribution. The corona ring model is developed and analysed in different dimensions. Optimisation algorithms that include GSA, ICA and GWO are applied to achieve the lowest electric field distribution along the insulator string by varying the dimensions of the corona ring. All three methods are not adopted for optimising the parameters in both models are the size and length of insulator

47

string. ICA and GSA were chosen for 33 kV and ICA and GWO were chosen for 132 kV for their optimisation elapsed time and the complexity of both models in FEA. GWO took about 183036.27 seconds to achieve the optimal results and about 309351. 25 seconds were taken using ICA in 132 kV model. For 33 kV insulator string, optimisation elapsed time was 301607.10 seconds only for 50 iterations. The best corona ring dimension results with the lowest electric field distribution are used to improve the insulator string model.

CHAPTER 4: RESULTS AND DISCUSSION

4.1 Introduction

This chapter performs the results that have been obtained from this work and discussion of the results. The results include the distribution of electric field and electric potential along the composite insulators, comparison between with and without corona ring and the proposed methods in optimising the design of the corona ring using optimisation algorithms.

4.2 Electric field and electric potential distributions along 33 kV insulator string

The distributions of electric field and potential around the energised end along the insulator were examined. Figures 4.1 and Figure 4.2 present the distributions of the electric potential and electric field obtained from the finite element analysis (FEA) 3-dimensional (3D) model geometry from the original dimensions of 33 kV insulator string. Figure 4.3 shows the contour of electric potential distribution with corona ring. It can be seen that the maximum electric field is obtained at the energised end where the corona ring is located. The maximum recommended electric field by IEEE task force is 4.5 kV/cm ("IEEE Guide for Application of Composite Insulators," 2002). The inclusion of a corona ring to the insulator has reduced the maximum electric field gradient along the insulator surface. This can reduce the corona effect, prolonging the life of the insulator and preventing excessive levels of radio interference (Niedospial, 2012; Wenxia Sima et al., 2006). However, the position of the corona ring at inappropriate locations on the insulator may lead to amplification of the maximum electric field.
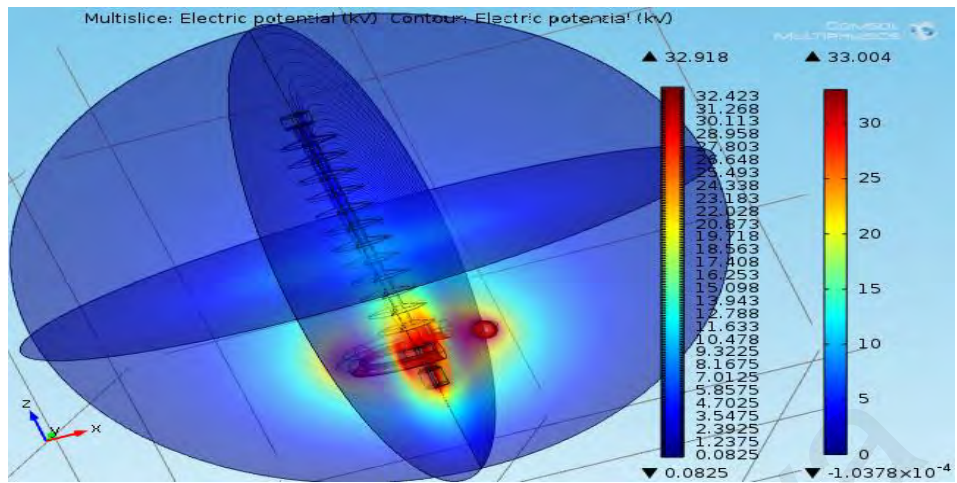
Figure 4.1: Electric potential distribution in the FEA model
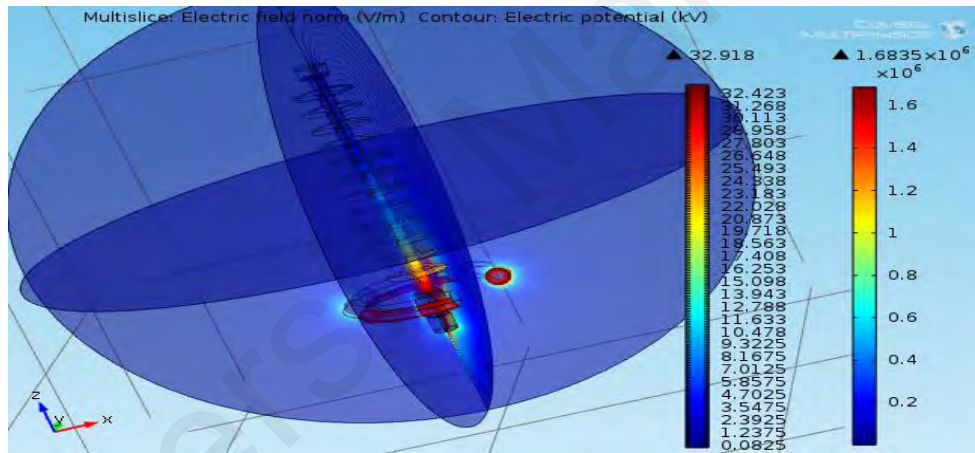
Figure 4.2: Electric field distribution in the FEA model
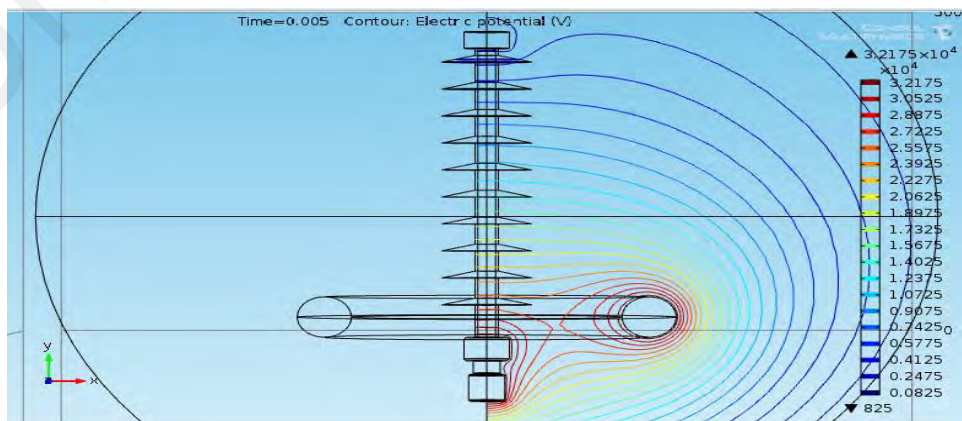
Figure 4.3: Contour of electric potential distribution with corona ring

**4.3	Effect of corona ring dimensions on 33 kV insulator string**

To observe the effect of the corona ring design on the electric field magnitude on the insulator string at point 122 (referring to Figure 3.1), different combinations of the ring diameter R, the ring tube diameter r and the vertical position H of the ring along the insulator string were assigned. Point 122 is the point on the insulator string surface nearest to the high voltage terminal. Each parameter was varied while keeping the other two parameters constant. The ring diameter R was varied between 60 mm and 150 mm while ring tube diameter r was varied between 5 mm and 50 mm. The vertical position of the ring H was kept constant at 0 m, which is at the position of the insulator high voltage point.

Tables 4.1 show the data collected from the simulation. Although the optimisations of the insulator design were focused on the point 122, few other points were also considered in this simulation for comparison purposed. The cells highlighted in red are the minimum electric field on the insulator surface below 4.5 kV/cm, which is the maximum electric field suggested by IEEE. From this simulation result, the lowest minimum value for the electric field is 3.059 kV/cm. This electric field magnitude was evaluated based on dimensions of corona ring diameter 120 mm, ring tube diameter 45 mm and the height of ring along the insulator was set 0 mm. All the parameters were set in mm unit in the model and converted to cm unit after the simulation in COMSOL Multiphysics.

Table 4.1: Results of electric field distribution on 33 kV insulator string with the variation of *R*; *H* = 0 and *r* from 5 mm to 50 mm

Ring Diameter, R (mm)	60	70	80	90	100	110	120	130	140	150	
Points (122) Electric field (kV/cm)	3.088	3.088	3.070	3.067	3.083	3.086	3.087	3.089	3.095	3.082	*r* = 5 mm
	3.084	3.101	3.092	3.084	3.083	3.096	3.070	3.096	3.073	3.075	*r* = 10 mm
	3.079	3.106	3.092	3.088	3.089	3.096	3.071	3.072	3.073	3.095	*r* = 15 mm
	3.096	3.089	3.086	3.084	3.103	3.080	3.102	3.083	3.078	3.079	*r* = 20 mm
	3.073	3.072	3.077	3.105	3.092	3.089	3.076	3.086	3.065	3.098	*r* = 25 mm
	3.081	3.092	3.085	3.080	3.099	3.082	3.078	3.097	3.082	3.077	*r* = 30 mm
	3.090	3.075	3.093	3.088	3.074	3.083	3.073	3.074	3.077	3.095	*r* = 35 mm
	3.096	3.069	3.107	3.079	3.076	3.083	3.081	3.089	3.091	3.095	*r* = 40 mm
	3.091	3.088	3.077	3.081	3.099	3.060	3.059	3.088	3.080	3.089	*r* = 45 mm
	3.081	3.083	3.085	3.094	3.080	3.082	3.108	3.084	3.071	3.075	*r* = 50 mm

Figure 4.4 shows the electric field magnitude at point 122 as a function of corona ring diameter when the ring tube diameter r was fixed at 45 mm. It can be seen that the electric field magnitude at point 122 decreases when the diameter of the corona ring is increased until R = 90 mm but increases after R = 90 mm. Figure 4.5 shows the electric field magnitude at point 122 as a function of the ring tube diameter r when the corona ring diameter R was fixed at 120 mm. When r is increased, the electric field magnitude at point 122 is smaller. Hence, the ring tube diameter r should be larger to minimise the electric field magnitude at point 122.
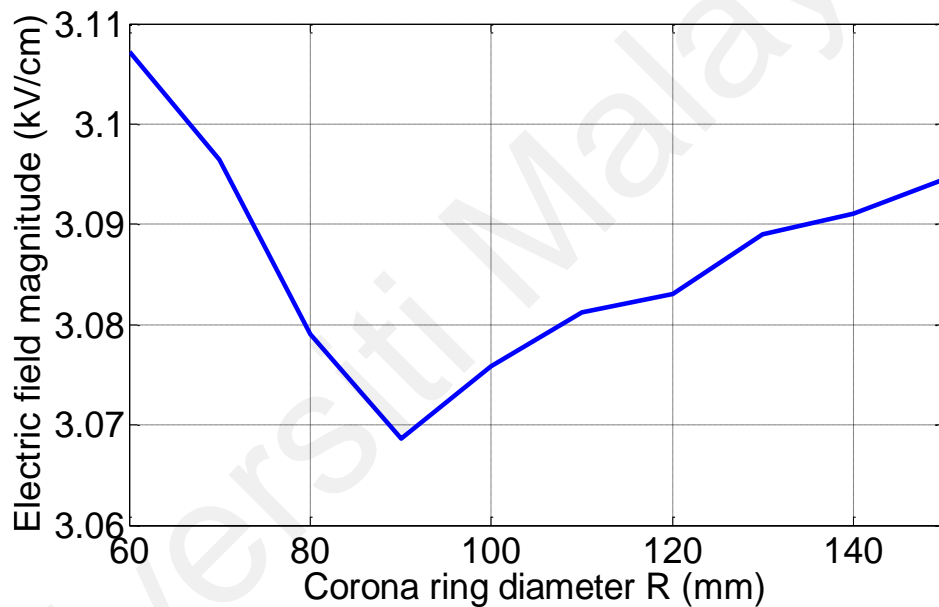
Figure 4.4: Electric field magnitude at point 122 as a function of corona ring diameter R (ring tube diameter r = 45 mm)
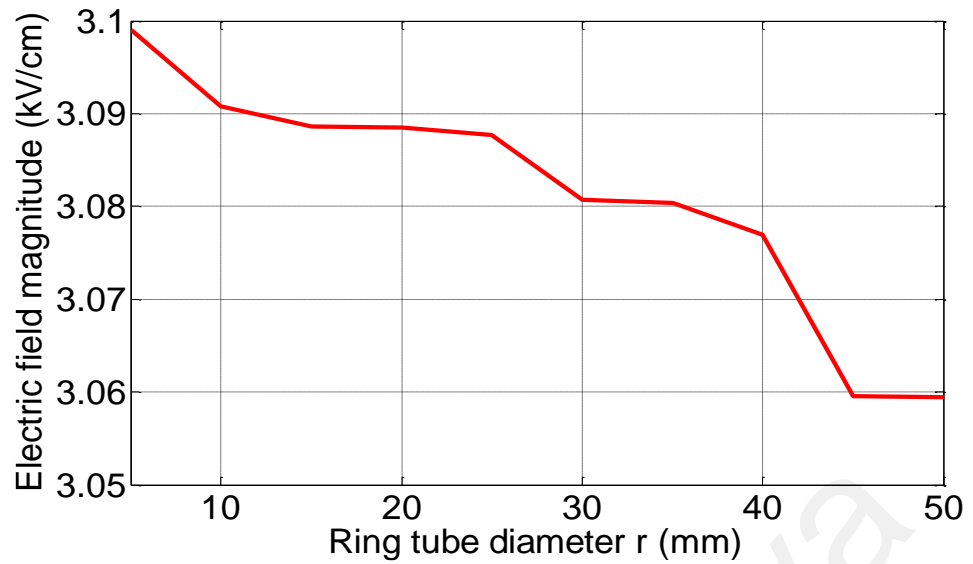
Figure 4.5: Electric field magnitude at point 122 as a function of ring tube diameter *r* (corona ring diameter *R* = 120 mm)

Figure 4.6 shows the electric potential lines in the insulator string model geometry with different ring tube diameters *r* and with *R* = 120 mm and *H* = 0 m. From this figure, it can be seen that the electric potential lines are different when the ring tube diameter is changed.
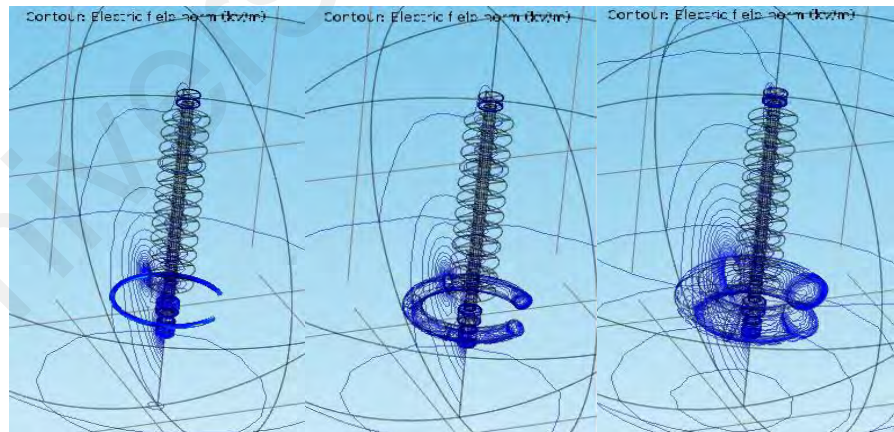
(a)   (b)   (c)

Figure 4.6: Electric potential lines in the model geometry with different tube diameters *r*; (a) 5 mm, (b) 20 mm and (c) 45 mm (*R* = 120 mm and *H* = 0 m)

4.4   Optimisation results using ICA and GSA for 33 kV insulator string

In this section, two different optimisation techniques, Gravitational Search Algorithm (GSA) and Imperialist Competitive Algorithm (ICA), were applied to obtain the optimum design of a corona ring on the insulator string model by minimising the electric field near the high voltage terminal. The results obtained using GSA and ICA are compared and discussed. In this section, only two techniques were applied in this model and other technique which is GWO is not used due to 3D model insulator string. Optimisation duration is longer using GWO in 3D model. The parameters of the corona ring set as variables for GSA and ICA are the ring diameter R, ring tube diameter r and the vertical position H of the ring along the insulator. The fitness function was set as the lowest electric field magnitude near the high voltage terminal of the insulator string, which is at point 122.

Three case studies of the optimisation were performed. For case 1, the parameter set as the variable is the corona ring tube diameter r. For case 2, the parameters set as the variables are the ring tube diameter r and corona ring diameter R. Finally, for the case 3, the ring tube diameter r, corona ring diameter R and the vertical position H of the ring along the insulator were set as the variables. The descriptions of all case studies are summarised in Table 4.2 while Figure 4.7 shows the parts that were set as the variables for each case study.

Table 4.2: Descriptions of each case study for optimisation methods

Case study	Parameter
Case 1	Ring tube diameter r
Case 2	Ring tube diameter r Ring diameter R
Case 3	Ring tube diameter r Ring diameter R Vertical position H of the ring along the insulator
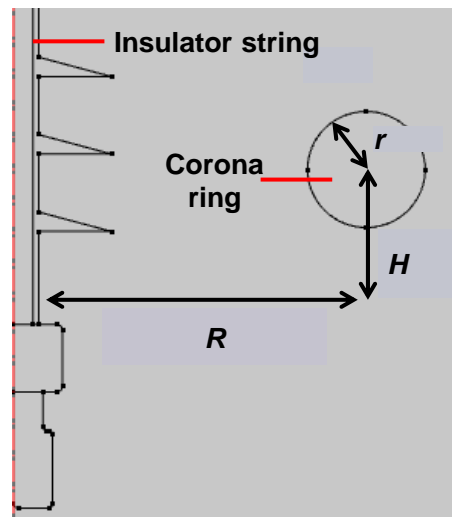
Figure 4.7: Parts set as the variables for each case study

Table 4.3 shows the lower and upper limits of each parameter used for the optimisation methods. The limits were fixed based on the limits relative to the insulator string dimensions. Table 4.4 shows parameters that were set for ICA and GSA used in this work.

Table 4.3: Lower and upper limits of each parameter used for optimisation method

Parameter	Lower limit	Upper limit
Ring tube diameter (mm)	$r_{min} = 5$	$r_{max} = 50$
Ring diameter (mm)	$R_{min} = 60$	$R_{max} = 150$
Vertical position of the ring along the insulator (mm)	$H_{min} = 0$	$H_{max} = 100$

Table 4.4: Parameters set for ICA and GSA

ICA	GSA
Number of iteration = 50	Number of iteration = 50
Number of population = 50	Number of population = 50
Assimilation constant $\beta = 2$	Gravitational constant power $\alpha = 10$
Total cost constant $\zeta = 0.02$	Gravitational constant initial value $G_o = 100$
Degree of revolution $P_{revolve} = 0.5$	Power of Euclidean distance $R_{power} = 1$

Table 4.5 shows the results obtained from the optimisation methods for all case studies. From these results, it can be seen that the electric field magnitude at point 122 is lower using optimisation methods, GSA and ICA, compared to without using optimisation techniques. Hence, this shows that the corona ring design of the insulator string has been successfully optimised using GSA and ICA. Comparison of the obtained results between GSA and ICA was also made. For Case 1, which the ring tube diameter r was set as the variable, it can be seen that the electric field magnitude obtained by GSA and ICA are quite similar. For Case 2, which the ring tube diameter r and ring diameter R were set as the variables, the results show that the electric field magnitude obtained using GSA is slightly less than ICA. For Case 3, which the ring tube diameter r, ring diameter R and the vertical position H of the ring along the insulator were set as the variables, the electric field magnitude obtained using GSA is also slightly less than ICA. Thus, this indicates that GSA is more suitable for optimising a corona ring design for an insulator string than ICA.

Also, referring to Table 4.5, comparison between three different cases shows that the optimisation methods for Case 3 yield the lowest electric field magnitude at point 122 in

the model geometry than Case 1 and Case 2. Hence, this indicates that when more variables are used for the optimisation methods, the solutions achieved are better.

Table 4.5: Optimised parameters using ICA and GSA

Case	Variables	Parameter values		Electric Field (kV/cm) at point 122		
		GSA	ICA	GSA	ICA	Without optimisation
1	r	49.937	49.999	2.435	2.471	3.059
2	r	49.859	50.000	2.422	2.464	3.059
	R	134.564	102.192			
3	r	43.437	45.615	0.382	0.980	3.059
	R	117.415	123.538			
	H	33.647	57.559			

Figure 4.8 shows the convergence curve against iteration for GSA and ICA. From this figure, it can be seen that the convergence for GSA is faster than ICA. GSA converges at iteration 12. Hence, GSA achieves the solutions faster than ICA for the optimum corona ring design of the insulator string model in this work.
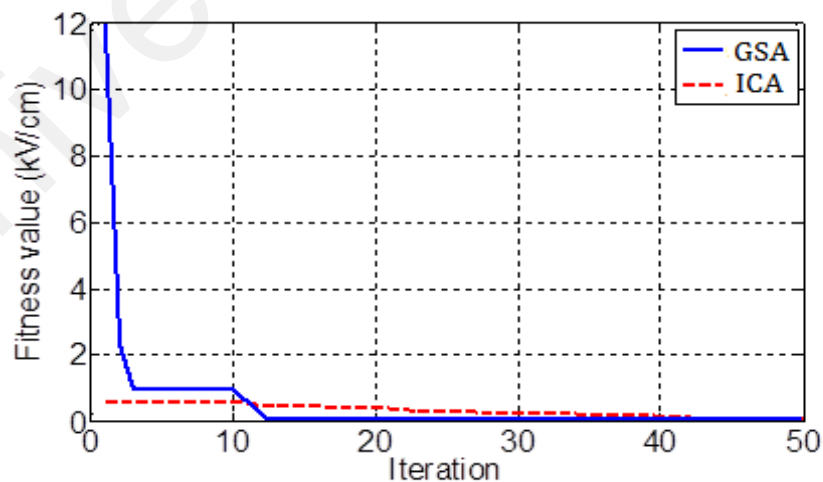
Figure 4.8: Convergence curve for GSA and ICA

4.5 Electric field and electric potential distributions along 132 kV insulator string

The simulation results for the 132 kV of insulator string with corona ring model that has been developed are presented in this section. The results of the electric potential and electric field distributions with and without corona ring were optimised using different dimensions and compared with the results using non-linear optimisation techniques. The distributions of electric field and electric potential around the energised end along the insulator are examined using COMSOL multiphysics. The comparisons have been done for the two-dimensional (2D) simulation models and the critical points affecting simulation accuracy are examined. In this geometry, the insulator system voltage is 132 kV and the basic insulation level (Nosratabadi et al.) is 650/750 kV. The total length of the insulator is 1650 mm and it has 40 weather sheds. It can be seen that the maximum electric field is obtained at the energised end where the corona ring is located. The maximum recommended electric field by IEEE task force is 4.5 kV/cm. The inclusion of corona ring to the insulator aids the system with lower corona effect, thus prolonging the life of the insulator, minimising the maximum electric field gradient along insulator surface and preventing excessive levels of radio interference (W. Sima, K. Wu, Q. Yang, & C. Sun, 2006). Figures 4.9 and Figure 4.10 show the electric potential and electric field distribution obtained from the FEA model geometry.

Figure 4.9: Electric potential distribution of an insulator after the simulation

Figure 4.10: Electric field distribution of an insulator after the simulation
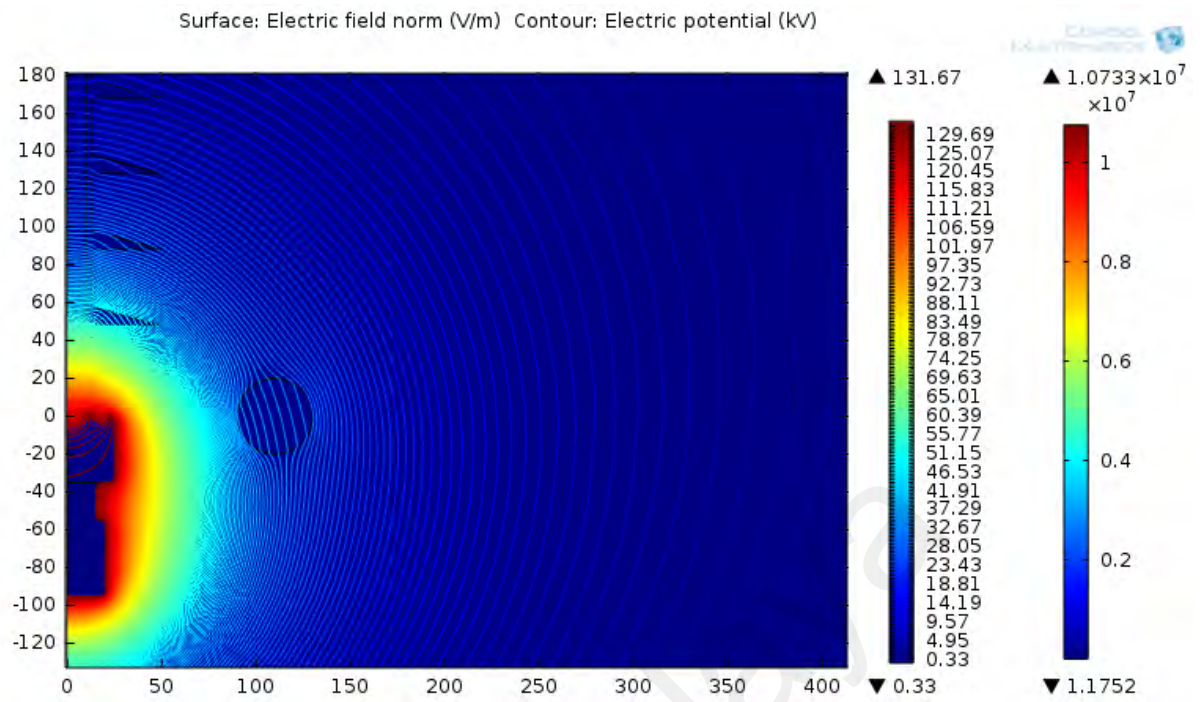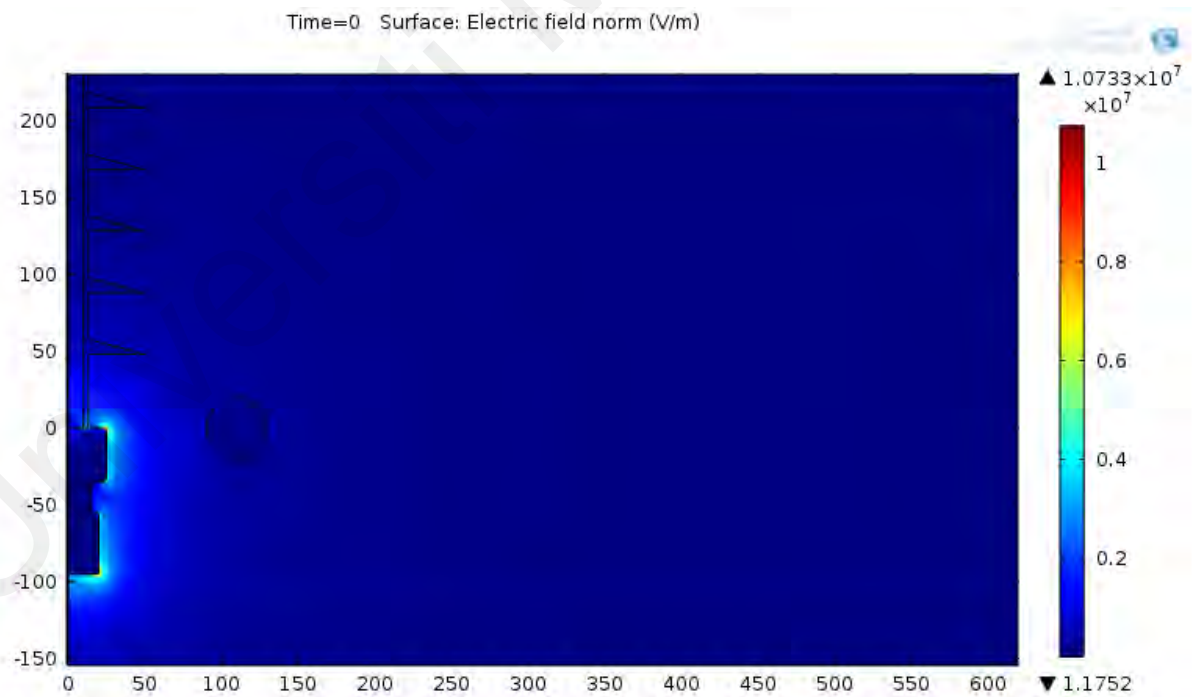
4.6 Simulation results using various parameter values of corona ring in 132 kV insulator string

To observe the effect of the three parameters on the design at point 116 (referring to Figure 3.2), the electric field was computed for practical values of R, r and H independently, while keeping the other two parameters as constants. In this section, the simulation processes were done for all the selected parameters. The results of the electric field [kV/cm] were collected. The variation of ring diameter, R is between the ranges of 60 mm and 150 mm, whereas the variation of diameter of ring tube, r is between 5 mm and 50 mm. The vertical position of the ring, H was kept constant at 0 for all the simulation steps. Figure 4.11 shows the selected point 116, along the surface of insulator string, where this is the point has high electric field without corona ring.

Table 4.6 shows the data collected from the simulation for minimum electric field with corona ring at point 116. Although the optimisations of the insulator design were focused on the point 116, few other points were taken also into account in this simulation for comparison.

The cells highlighted in red in Table 4.6 are the electric field on the insulator surface below 4.5 kV/cm, where 4.5 kV/cm is the maximum electric field suggested by IEEE task force in (Phillips et al., 2008). From this simulation result, the lowest minimum value for the electric field is 3.827 kV/cm with the optimal dimensions; R is 80 mm, r is 25 mm and H is 0. However, some values from the Table 4.6 are not considered even though the values are below 3.827 kV/cm such as 3.658 kV/cm ($R = 90$ mm and $r = 35$ mm) and 3.619 kV/cm ($R = 100$ mm and $r = 45$ mm). This is because the corona ring is overlapping the insulator as in Figure 4.12, which should be considered. Apart from that, N/A in Table 4.6 also showed that those values cannot be evaluated due to the corona ring overlapping the insulator string.
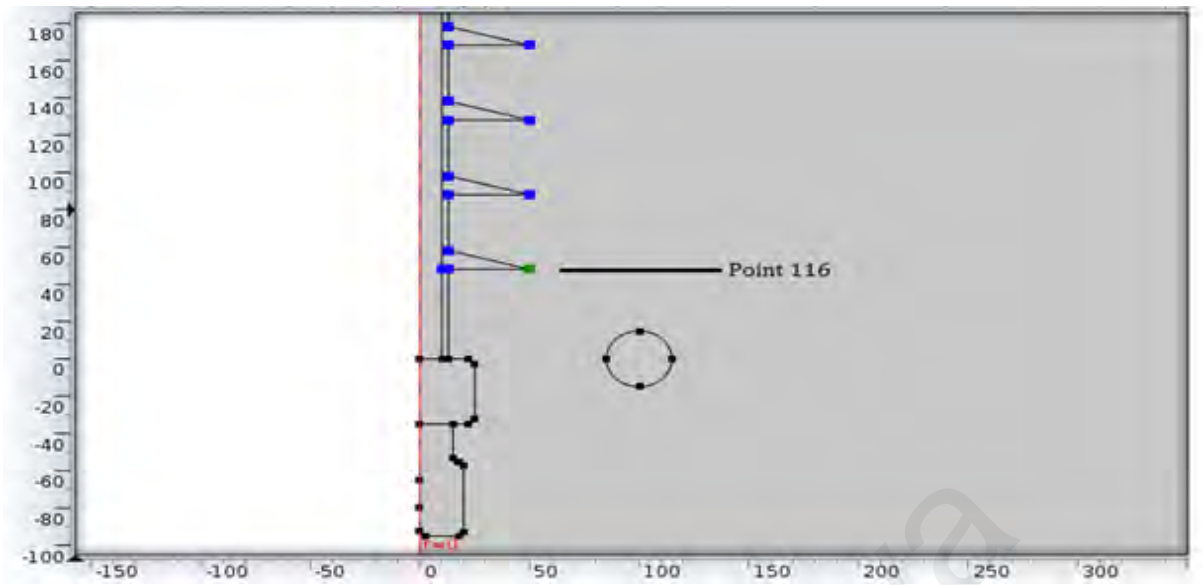
Figure 4.11: Selected point along the insulator

Figure 4.12: Overlapping corona ring along insulator string

Table 4.6: Results of electric field distribution on 132 kV insulator string with the variation of *R*: *H*=0 and *r* from 5 mm to 50 mm

Ring Diameter, R (mm)	60	70	80	90	100	110	120	130	140	150	
	4.314	4.325	4.333	4.338	4.348	4.354	4.356	4.356	4.355	4.359	*r* = 5 mm
	4.299	4.219	4.265	4.303	4.331	4.346	4.355	4.356	4.356	4.362	*r* = 10 mm
	13.967	4.086	4.162	4.252	4.289	4.327	4.344	4.363	4.364	4.365	*r* = 15 mm
	17.757	11.700	4.010	4.161	4.248	4.313	4.341	4.361	4.366	4.373	*r* = 20 mm
Points (116) Electric field (kV/cm)	24.604	14.296	3.827	4.021	4.156	4.283	4.331	4.354	4.378	4.379	*r* = 25 mm
	37.636	18.451	11.923	3.866	4.077	4.231	4.319	4.361	4.387	4.393	*r* = 30 mm
	67.285	25.481	14.739	3.658	3.968	4.125	4.305	4.359	4.387	4.405	*r* = 35 mm
	N/A	39.141	18.650	12.110	3.802	4.104	4.277	4.346	4.399	4.409	*r* = 40 mm
	N/A	70.143	25.970	14.866	3.619	3.954	4.208	4.324	4.392	4.431	*r* = 45 mm
	N/A	N/A	41.386	18.944	12.132	3.808	4.099	4.260	4.356	4.399	*r* = 50 mm

The simulation results show that the maximum electric field is not always at point 116, but it changes according to the position and dimensions of the corona ring. The closer the ring to the insulator, the lower the fields in the region close to the end-fitting. However, the field on the sheath away from the end-fitting is higher for smaller diameters. Increasing or decreasing the ring diameter has a smaller impact on the electric field at the energised end compared to the ring position.

From Figure 4.13, it can see that the electric field at point 116 is reduced when the diameter of ring tube, r is increased.
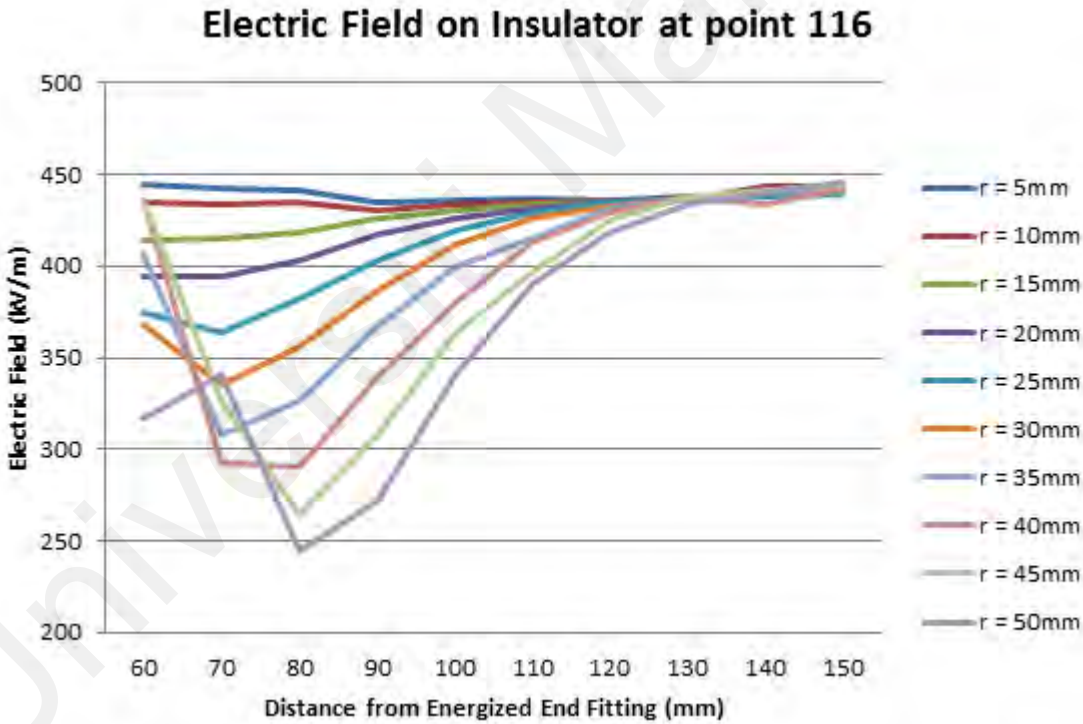
Figure 4.13: Electric field at point 116 for the variation of r and R

Contour graphs are shown in Figure 4.14 the contour graphs show variation of diameter of the ring tube, r and the changes of the electric field.

| r = 5 mm | r = 25 mm | r = 45 mm |
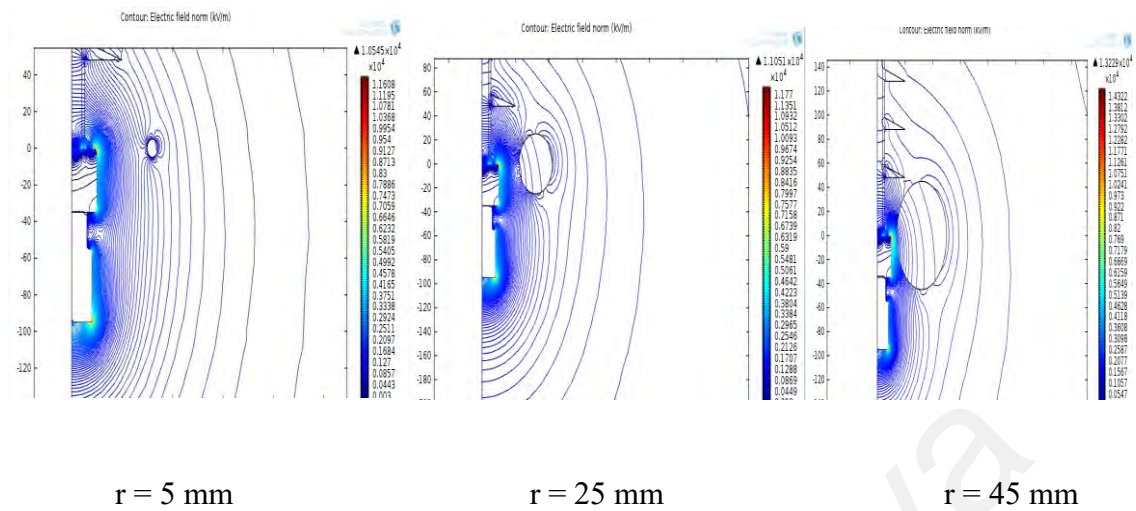
Figure 4.14: Contour graphs for variation diameter of ring tube, *r*

4.7   Optimisation results using ICA and GWO for 132 kV insulator string

In this section, two different non-linear optimisation techniques, Imperialist Competitive Algorithm (ICA) and Grey Wolf Optimisation (GWO) were used to obtain the minimum electric field magnitude for 132 kV insulator string. For this model, GSA technique is not applied because its optimisation results are not suitable for higher applied voltage. The results obtained from the FEA model of the insulator string with corona ring were interfaced with MATLAB programming code to evaluate the objective function. The results from ICA and GWO are compared and explained. There are few dimensions used on corona ring and insulator string. The important ring dimensions in corona ring design are ring diameter *R*, diameter of ring tube *r* and vertical position of the ring along the insulator *H* of the insulator. These parameters are optimised by ICA and GWO in order to achieve the lowest electric field along insulator string.

Three case studies of the optimisation were done. For case 1, the dimension needs to be optimised is diameter of ring tube, r. For case 2, the dimensions for both diameter of ring tube, r and ring diameter, R of corona ring are optimised. For case 3, diameter of ring tube, r, ring diameter, R and height of the ring, H. The descriptions of all case studies are summarised in Table 4.7 while Figure 4.15 shows the materials and domains that were optimised.

Table 4.7: Description of the case studies using optimisation techniques

Case	Parameter: Description
Case 1	Diameter of ring tube, r
Case 2	Diameter of ring tube, r Ring diameter, R
Case 3	Diameter of ring tube, r Ring diameter, R Vertical position of the ring along the insulator, H
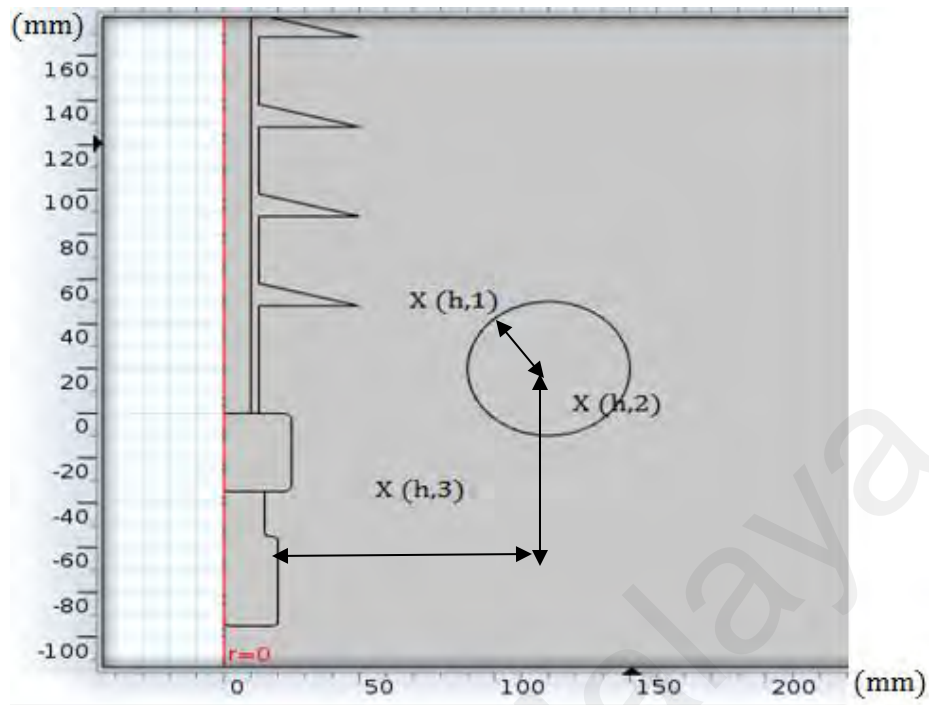
Figure 4.15: Optimised parameters of insulator and corona ring

The lower and upper limit of every parameter are fixed based on the limits relative to the ring dimension as shown in Table 4.8. The number of iterations used in ICA and GWO is 100. Figure 4.16 and Figure 4.17 show the results after 100 iterations for both optimisation methods. GWO achieved the solution at iteration 56 while ICA at iteration 72. Hence, GWO achieves the best solutions faster than ICA for the optimum corona ring design of the insulator string model in this work.

Table 4.8: Lower and upper limit of each parameter used in optimisation

Parameter	Lower limit	Upper limit
Diameter of ring tube (mm)	$r_{min} = 5$	$r_{max} = 50$
Ring diameter (mm)	$R_{min} = 60$	$R_{max} = 150$
Vertical position of the ring along the insulator (mm)	$H_{min} = 0$	$H_{max} = 100$
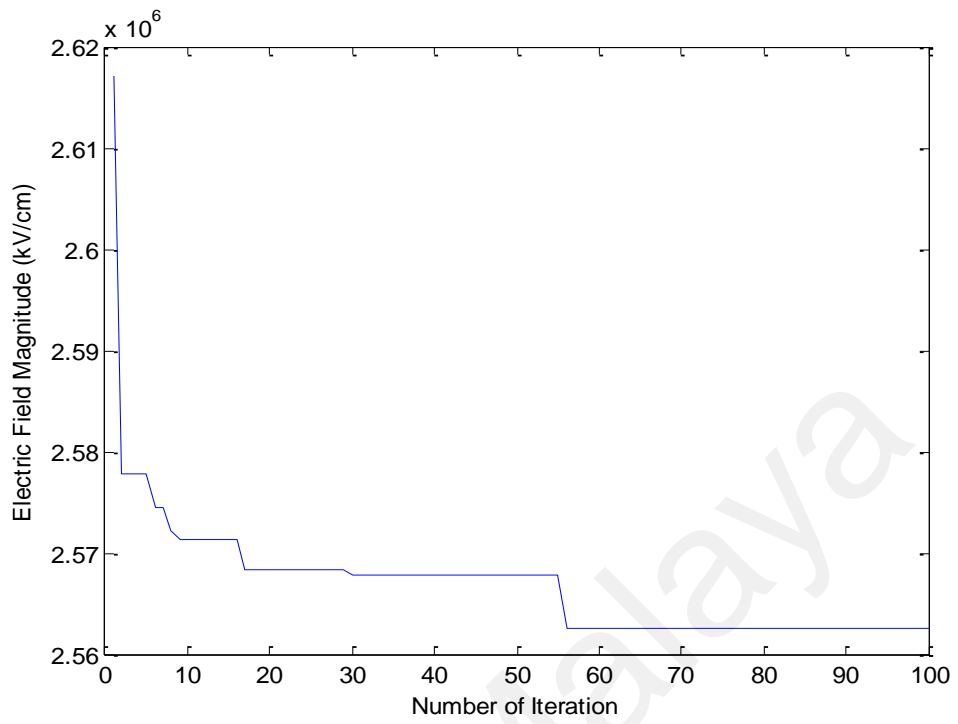
Figure 4.16: Simulation results for GWO after 100 iterations
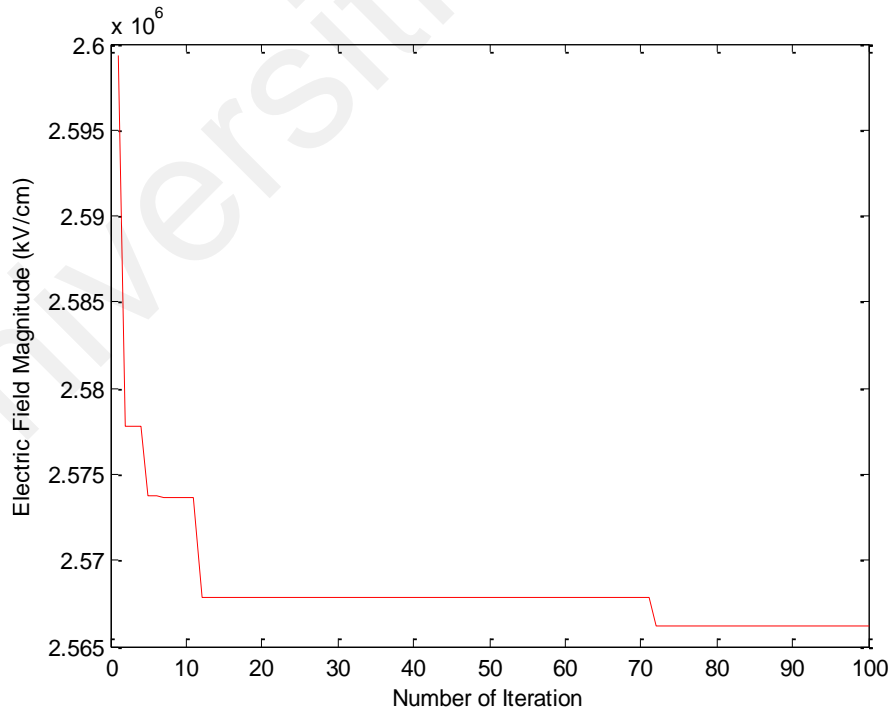
Figure 4.17: Simulation results for ICA after 100 iterations

Table 4.9 shows the results for all three case studies. For case 1, which is varying diameter of ring tube, it can be seen that the electric fields obtained by ICA and GWO are quite similar. In Case 1, the diameter of ring tube value of both techniques is the same. Case 2 shows the result of varying the ring diameter of the corona ring. The electric field obtained using GWO is lower than ICA while for Case 3, it shows the vertical position of the ring along the insulator in ICA is higher than GWO.

Table 4.9: Optimised parameters using ICA and GWO

Case	Optimised parameters	Parameter Values (mm)		Electric Fields at Point 116 (kV/cm)		Without optimisation
		ICA	GWO	ICA	GWO	
Case 1	r	24.114	24.101	3.871	3.859	3.827
Case 2	r	23.999	24.220	3.920	3.899	3.827
	R	82.145	81.370			
Case 3	r	25.112	24.897	3.777	3.724	3.827
	R	83.147	82.181			
	H	21.718	20.978			

The comparison is made between ICA and GWO, which have been used to obtain the optimum dimensions and the minimum electric field on the insulator string. From the result, GWO optimisation technique gives better results compared to ICA optimisation technique. All of the three parameters; r, R and H have lower values in GWO compared to ICA method. The minimum electric field obtained from Case 3 is compared to Case 1 and

Case 2. From the comparison using GWO method, the electric field from the optimised results is about 10.3% lower than without the optimisation.

Finally, the optimum dimensions of the corona ring, which yield the lowest electric field were identified, which are $R = 82.181$ mm, $r = 24.897$ mm and $H = 20.978$ mm. Figure 4.18 shows the simulation results with the optimum dimensions, where the minimum electric field simulated is 3.724 kV/cm.
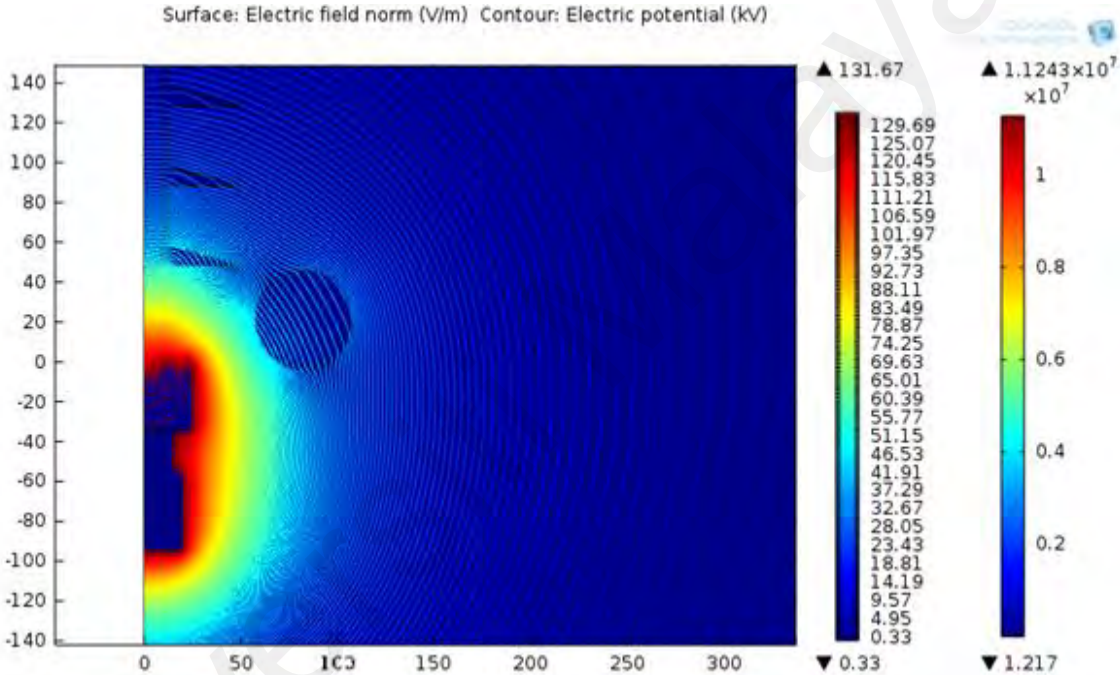
Figure 4.18: Optimal dimensions and minimum electric field

4.8   Summary of the chapter

In this chapter, the simulation results that have been obtained from this work were analysed and discussed. These include the simulation results of corona ring dimensions, optimisation results and comparison of minimum electric field between with corona ring and without corona ring along the insulator string. From the optimisation results, GSA

yields better results in reducing the electric field along the insulator string than ICA for 33 kV insulator string. GWO achieves better solutions and faster than ICA for the optimum corona ring design of 132 kV insulator string model in this work. Since 33 kV insulator string were modeled in 3D, the number of iterations were set to 50. While 132 kV with 2D model were increased to 100 iterations. This difference was made due to the iteration time taken between the two models. The effectiveness of the optimised design of corona ring is verified by developing the model in FEA software for different settings and conditions.

CHAPTER 5: CONCLUSIONS AND RECOMMENDATIONS

5.1   Conclusions

In this work, the effect of different dimensions of corona ring along the insulator string and distributions of electric field has been successfully evaluated using simulation models. A three-dimensional 33 kV and two-dimensional 132 kV non-ceramic insulator model geometry has been successfully developed with and without corona ring in finite element analysis (FEA) software to evaluate the electric field distribution. From the results, it was found that the implementation of a corona ring onto the insulator string can reduce the electric field significantly at the energised end of the insulation string. This is due to the corona ring causes high electric field to be re-distributed towards the unenergised end of the insulator string. The electric field distribution on the insulator string depends on the corona ring diameter, the ring tube diameter and the vertical position of the ring along the insulator string. Thus, the proposed FEA model for corona ring modelling along insulator string in this work can be considered reasonable.

Three optimisation techniques were successfully implemented in this work to obtain the optimum design of the corona ring on the insulator string in two different insulator operating voltage. Using optimisation techniques, lower electric field magnitude at the energised end of the insulation string is obtained compared to without using optimisation techniques. Comparison between the three optimisation methods shows that Gravitational Search Algorithm (GSA) yields a lower minimum electric field magnitude and converges faster than Imperialist Competitive Algorithm (ICA) along 33 kV insulator string. This is due to GSA achieves the solutions faster than ICA. Whereas Grey Wolf Optimisation (GWO) yields the minimum electric field magnitude and converges faster than Imperialist

Competitive Algorithm (ICA) along 132 kV insulator string. This is due to GWO achieves the solutions faster than ICA. Hence, GSA and GWO are recommended for optimisation of corona ring design on insulator strings for different level of voltage.

5.2   Recommendations

Recommendations for the future work are as follows:

1) Laboratory testing to verify the simulation results. The electric field distribution results, simulation results and optimisation results of the insulator string model can be obtained and the comparison between the measurement and simulation results can be done.

2) In this study, the best optimisation design of the corona ring is focusing on reducing the distribution of electric field along the insulator string. However, the simulation model also can be improved by including the effect of corona ring dimensions due to different environment and natural problem. By adding the layer of pollution along the insulator and installing optimal dimension of corona ring, the minimum electric field distribution can be obtained. Also, the simulation model can be improved by increasing number of parameters to be optimised such as the permittivity of the insulator.

REFERENCES

Akbari, E., Mirzaie, M., Rahimnejad, A., & Asadpoor, M. (2012). *Finite Element Analysis of Disc Insulator Type and Corona Ring Effect on Electric Field Distribution over 230-kV Insulator Strings* (Vol. 1).

Araya, J., Montaña, J., & Schurch, R. (2021). *Electric Field Distribution and Leakage Currents in Glass Insulator Under Different Altitudes and Pollutions Conditions using FEM Simulations.* IEEE Latin America Transactions, 19(8), 1278-1285.

Arshad, Nekahi, A., McMeekin, S., & Farzaneh, M. (2015). *Influence of Voltage Type and Polarity on Electric field distribution along a Polymeric Insulator under Contaminated Conditions.*

Arumugam, S., Haba, Y., Koerner, G., Uhrlandt, D., & Paschen, M. (2018). *Understanding partial discharges in low-power relay and silicone cable modified to suit high-voltage requirement of deep sea electrical system.* International Transactions on Electrical Energy Systems, 28(6), e2542.

Atashpaz-Gargari, E., & Lucas, C. (2007, 25-28 Sept. 2007). *Imperialist competitive algorithm: An algorithm for optimization inspired by imperialistic competition.* Paper presented at the 2007 IEEE Congress on Evolutionary Computation.

Bakar, A., Abidin, A., Illias, H., Mokhlis, H., Abd Halim, S., Hassan, N., & Tan, C. K. (2016). *Determination of the striking distance of a lightning rod using finite element analysis.* Turkish Journal of Electrical Engineering & Computer Sciences, 24, 4083-4097.

Bashiri, M., & Bagheri, M. (2012). *Using Imperialist competitive algorithm optimization in multi-response nonlinear programming.* International Journal of Industrial Engineering & Production Research, 24.

Chao, Y., & Huang, F. (2019). *Preliminary study on icing and flashover characteristics of inverted T-type insulator strings.* Electrical Engineering, 101(3), 675-683.

Chen, J., & Imani Marrani, H. (2020). *An Efficient New Hybrid ICA-PSO Approach for Solving Large Scale Non-convex Multi Area Economic Dispatch Problems.* Journal of Electrical Engineering & Technology, 15(3), 1127-1145.

Cherney, E. A. (2005). *Silicone rubber dielectrics modified by inorganic fillers for outdoor high voltage insulation applications.* IEEE Transactions on Dielectrics and Electrical Insulation, 12(6), 1108-1115.

Daochun, H. (2013). *Study on parameters design and corona characteristics test equivalent of grading rings for 1000kV UHV AC compact transmission line.* Conference on Electrical Insulation and Dielectric Phenomena (CEIDP). IEEE.

Deng, T., Li, Q. F., Zhang, X. J., Su, Z. Y., & Fan, J. B. (2009). *The optimization of grading ring design for ±800 kV UHV DC transmission lines* (Vol. 29).

Dhavakumar, P., & Gopalan, N. P. (2021). *An efficient parameter optimization of software reliability growth model by using chaotic grey wolf optimization algorithm.* Journal of Ambient Intelligence and Humanized Computing, 12(2), 3177-3188.

Diako Azizi, A. G., Alireza Siadatan. (2012). *Corona ring optimization for different cases of polymer insulators based on its size and distance,* 1(2).

Dominguez, D. C., Espino-Cortes, F. P., & Gomez, P. (2013). *Optimized design of electric field grading systems in 115 kV non-ceramic insulators.* IEEE Transactions on Dielectrics and Electrical Insulation, 20(1), 63-70.

Domínguez, D. C., Espino-Cortés, F. P., & Gómez, P. (2011, 5-8 June 2011). *Optimization of electric field grading systems in non-ceramic insulators.* Paper presented at the 2011 Electrical Insulation Conference (EIC).

Dutta, P., & Nayak, S. K. (2021). *Grey Wolf Optimizer Based PID Controller for Speed Control of BLDC Motor.* Journal of Electrical Engineering & Technology, 16(2), 955-961.

Electric fields on AC composite transmission line insulators. (2008). *IEEE Taskforce on Electric Fields and Composite Insulators, Power Delivery,* IEEE Transactions on.

Eleperuma, K., Saha, T. P., & Gillespie, T. (2008). *Electric field modelling of non–Ceramic high voltage insulators.* Australian Journal of Electrical and Electronics Engineering, 4(3), 239-248.

Esmat Rashedi, Hossein Nezamabadi-pour , & Saryazdi, S. (2009). *GSA: A Gravitational Search Algorithm.* Information Sciences, 179, 2232–2248.

Farzaneh, M., & Chisholm, W. (2009). *Insulators for Icing and Polluted Environments.* Wiley-IEEE Press.

Gubanski, S. M. (2005). *Modern outdoor insulation - concerns and challenges.* IEEE Electrical Insulation Magazine, 21(6), 5-11.

Gui-qing, R. (2009). *Design of Grading Rings for 1000kV AC Composite Insulator.* High Voltage Engineering.

Hall, J. F. (1993). *History and bibliography of polymeric insulators for outdoor applications.* Power Delivery, IEEE Transactions, 8(1), 376-385.

hamdi, B. M., Teguar, M., & Mekhaldi, A. (2013, 30 June-4 July 2013). *Potential and electric field distributions on HV insulators string used in the 400 kV novel transmission line in Algeria.* Paper presented at the 2013 IEEE International Conference on Solid Dielectrics (ICSD).

Han, Y., & Tong, X. (2020). *Multi-Step Short-Term Wind Power Prediction Based on Three-level Decomposition and Improved Grey Wolf Optimization.* IEEE Access, 8, 67124-67136.

Hassanzadeh, H. R., & Rouhani, M. (2010). *A Multi-objective Gravitational Search Algorithm*. 2nd International Conference on Computational Intelligence, Communication Systems and Networks, 2010, pp. 7-12.

He, J., & Gorur, R. S. (2014). *Charge simulation based electric field analysis of composite insulators for HVDC lines.* IEEE Transactions on Dielectrics and Electrical Insulation, 21(6), 2541-2548.

IEEE Guide for Application of Composite Insulators. (2002). *IEEE Std 987-2001 (Revision of IEEE Std 987-1985)*, 1-24.

Ilhan, S., & Ozdemir, A. (2007). *Effects of Corona Ring Design on Electric Field Intensity and Potential Distribution Along An Insulator String.* 7th International Conference on Electrical and Electronics Engineering ELECO'07, Volume: Vol. 1 pp:142-146.

Illias, H. A., Abd Halim, S., Abu Bakar, A. H., & Mokhlis, H. (2015). *Determination of surge arrester discharge energy using finite element analysis method.* IET Science, Measurement & Technology, 9(6), 693-701.

Illias, H. A., Chean, Y. S., Ling, L. Y., Mokhlis, H., Ariffin, A. M., & Yousof, M. F. M. (2021, 12-14 July 2021). *Corona Ring Design Impact on the Electric Field Distribution Surrounding an Insulator String.* Paper presented at the 2021 IEEE International Conference on the Properties and Applications of Dielectric Materials (ICPADM).

Illias, H. A., Mou, K. J., & Bakar, A. H. A. (2017). Estimation of transformer parameters from nameplate data by imperialist competitive and gravitational search algorithms. *Swarm and Evolutionary Computation, 36*, 18-26.

Ing, K. G., Mokhlis, H., Illias, H. A., Aman, M. M., & Jamian, J. J. (2015). *Gravitational Search Algorithm and Selection Approach for Optimal Distribution Network Configuration Based on Daily Photovoltaic and Loading Variation.* Journal of Applied Mathematics, 2015, 894758.

Insulator, P. (2013). *PLP Insulator for Power Transmission & Distribution Networks.* PLP Prefprmed Line Products.

Kim, D. H., Abraham, A., & Cho, J. H. (2007). *A hybrid genetic algorithm and bacterial foraging approach for global optimization.* Inf. Sci., 177(18), 3918–3937.

Kumar, S. M., & Kalaivani, L. (2014, 20-21 March 2014). *Electric field distribution analysis of 110 kV composite insulator using Finite Element Modeling.* Paper presented at the 2014 International Conference on Circuits, Power and Computing Technologies [ICCPCT-2014].

Liaoning Mec Group CO, L. (2012). *Composite Insulator Catalogue.*

M'Hamdi, B., Benmahamed, Y., Teguar, M., Taha, I. B. M., & Ghoneim, S. S. M. (2022). *Multi-Objective Optimization of 400 kV Composite Insulator Corona Ring Design.* IEEE Access, 10, 27579-27590.

Miao, D., Chen, W., Zhao, W., & Demsas, T. (2020). *Parameter estimation of PEM fuel cells employing the hybrid grey wolf optimization method.* Energy, 193, 116616.

Mirjalili, S., Mirjalili, S. M., & Lewis, A. (2014). *Grey Wolf Optimizer.* Advances in Engineering Software, 69, 46-61.

Mohammad, S. N., Hoseini, H. F., Mahdi, M. I. M., & Tavakoli, M. (2013). *Electric Field Distributions around Silicon Rubber Insulators in Polluted and Cleaned Area.*

Moreno, V. M., & Gorur, R. S. (1999). *AC and DC performance of polymeric housing materials for HV outdoor insulators.* IEEE Transactions on Dielectrics and Electrical Insulation, 6(3), 342-350.

Murawwi, E. A., & El-Hag, A. (2011, 15-17 Nov. 2011). *Corona ring design for a 400 kV non-ceramic insulator.* Paper presented at the 2011 2nd International Conference on Electric Power and Energy Conversion Systems (EPECS).

Naserbegi, A., Aghaie, M., & Zolfaghari, A. (2020). *Implementation of Grey Wolf Optimization (GWO) algorithm to multi-objective loading pattern optimization of a PWR reactor.* Annals of Nuclear Energy, 107703.

Nicolopoulou, E., Gralista, E., Kontargyri, V., Gonos, I., & Stathopulos, I. (2011). *Electric Field and Voltage Distribution Around Composite Insulators.* 17th International Symposium on High-Voltage Engineering (ISH 2011).

Niedospial, E. (2012, 7-10 May 2012). *Design and application of corona and grading rings for composite insulators.* Paper presented at the PES T&D 2012.

Nosratabadi, S., Szell, K., Beszedes, B., Imre, F., Ardabili, S., & Mosavi, A. (2020, 14-15 Oct. 2020). *Comparative Analysis of ANN-ICA and ANN-GWO for Crop Yield Prediction.* Paper presented at the 2020 RIVF International Conference on Computing and Communication Technologies (RIVF).

Onchantuek, W., & Oonsivilai, A. (2008). *Electric Field and Potential Distributions along Surface of Silicone Rubber Polymer Insulators Using Finite Element Method.* International Journal of Electrical and Computer Engineering, 2, 1055-1060.

Onchantuek, W., & Oonsivilai, A. (2009). *Electric Field and Potential Distributions along Surface of Silicone Rubber Polymer Insulators Using Finite Element Method.* World Academy of Science, Engineering and Technology 42.

Phillips, A. J., Childs, D. J., & Schneider, H. M. (1999). *Water drop corona effects on full-scale 500 kV non-ceramic insulators.* IEEE Transactions on Power Delivery, 14(1), 258-265.

Phillips, A. J., Kuffel, J., Baker, A., Burnham, J., Carreira, A., Cherney, E., Yu, J. (2008). *Electric Fields on AC Composite Transmission Line Insulators.* IEEE Transactions on Power Delivery, 23(2), 823-830.

Puri, V., Chauhan, Y. K., & Singh, N. (2015, 21-22 Dec. 2015). *Design optimization of permanent magnet synchronous machine for vertical axis wind turbine using gravitational search algorithm.* Paper presented at the 2015 2nd International Conference on Recent Advances in Engineering & Computational Sciences (RAECS).

Qi-ying, X., & Yong-sheng, Z. (2011, 8-10 Aug. 2011). *Research on corona ring setting and structure optimization of composite insulator based on neural network.* Paper presented at the 2011 2nd International Conference on Artificial Intelligence, Management Science and Electronic Commerce (AIMSEC).

Rahimnejad, A., & Mirzaie, M. (2012). *Optimal Corona Ring Selection for 230 kV Ceramic I-string Insulator using 3D Simulation.* International Journal of Scientific and Engineering Research 3(7):1-6.

Raj, S., & Bhattacharyya, B. (2018). *Reactive power planning by opposition-based grey wolf optimization method.* International Transactions on Electrical Energy Systems, 28(6), e2551.

Ramadhani, F., Hussain, M. A., Mokhlis, H., & Hajimolana, S. (2017). *Optimization strategies for Solid Oxide Fuel Cell (SOFC) application: A literature survey.* Renewable and Sustainable Energy Reviews, 76, 460-484.

Rashedi, E., Nezamabadi-pour, H., & Saryazdi, S. (2011). *Filter modeling using gravitational search algorithm.* Engineering Applications of Artificial Intelligence, 24(1), 117-122.

Rashtchi, V., Rahimpour, E., & Shahrouzi, H. (2012). *Model reduction of transformer detailed R-C-L-M model using the imperialist competitive algorithm.* Electric Power Applications, IET, 6, 233-242.

Ross, A. (1987). *High-voltage polymeric insulated cables.* Power Engineering Journal, 1(1), 51-59.

Rout, U. K., Sahu, R. K., & Panda, S. (2013, 20-21 March 2013). *Gravitational Search Algorithm based Automatic Generation Control for interconnected power system.* Paper presented at the 2013 International Conference on Circuits, Power and Computing Technologies (ICCPCT).

Sabri, N. M., Puteh, M., & Mahmood, M. R. (2013, 19-20 Aug. 2013). *An overview of Gravitational Search Algorithm utilization in optimization problems.* Paper presented at the 2013 IEEE 3rd International Conference on System Engineering and Technology.

Sahu, A., Sahoo, R., & Karmakar, S. (2021, 5-6 Oct. 2021). *The Study of Electric Field and Partial Discharges on XLPE Insulation under DC High Voltage using COMSOL Multiphysics.* Paper presented at the 2021 3rd International Conference on High Voltage Engineering and Power Systems (ICHVEPS).

Schümann, U., Barcikowski, F., Schreiber, M., C. Kärner, H., & M. Seifert, J. (2002). *FEM Calculation and Measurement of the Electrical Field Distribution of HV Composite Insulator Arrangements.* 39th CIGRE of HV Composite Insulator Arrangements.

Sebestyn, I. (2002). *Electric-field calculation for HV insulators using domain-decomposition method.* IEEE Transactions on Magnetics, 38(2), 1213-1216.

Shan, Z. (1997). *Calculation and Analysis of Electric Field Distribution along Composite Insulators.* Ms. D Dissertation, Dept Electrical Eng, Univ Tsinghua.

Shirkouhi, S. N., Eivazy, H., Ghodsi, R., Rezaie, K., & Atashpaz-Gargari, E. (2010). *Solving the integrated product mix-outsourcing problem using the Imperialist Competitive Algorithm.* Expert Syst. Appl., 37, 7615-7626.

Sima, W., Espino-Cortes, F. P., Cherney, E. A., & Jayaram, S. H. (2004, 19-22 Sept. 2004). *Optimization of corona ring design for long-rod insulators using FEM based computational analysis.* Paper presented at the Conference Record of the 2004 IEEE International Symposium on Electrical Insulation.

Sima, W., Wu, K., Yang, Q., & Sun, C. (2006). *Corona Ring Design of ±800kV DC Composite Insulator Based on Computer Analysis.* 2006 IEEE Conference on Electrical Insulation and Dielectric Phenomena, 457-460.

Sima, W., Wu, K., Yang, Q., & Sun, C. (2006, 15-18 Oct. 2006). *Corona Ring Design of Â±800kV DC Composite Insulator Based on Computer Analysis.* Paper presented at the 2006 IEEE Conference on Electrical Insulation and Dielectric Phenomena.

Soroudi, A., & Ehsan, M. (2012). *Imperialist competition algorithm for distributed generation connections.* Generation, Transmission & Distribution, IET, 6, 21-29.

Stefanini, D., Seifert, J. M., Clemens, M., & Weida, D. (2010, 23-27 May 2010). *Three dimensional FEM electrical field calculations for EHV composite insulator strings.* Paper presented at the 2010 IEEE International Power Modulator and High Voltage Conference.

Suat Ilhan, A. O. (2007). *Effects of corona ring design on electric field intensity and potential distribution along and insulator string.* Electrical Engineering Department, Istanbul, Turkey.

Subcommittee, E. (2002). *Minimum number of good (healthy) porcelain or glass insulator units in a string for live work.* IEEE Transactions on Power Delivery, 17(3), 809-814.

Taherian, R. (2019). *6 - Application of Polymer-Based Composites: Polymer-Based Composite Insulators*. In R. Taherian & A. Kausar (Eds.),* Electrical Conductivity in Polymer-Based Composites (pp. 131-181): William Andrew Publishing.

Tonmitr, N., Tonmitr, K., & Kaneko, E. (2016). *The Effect of Controlling Stray and Disc Capacitance of Ceramic String Insulator in the Case of Clean and Contaminated Conditions.* Procedia Computer Science, 86, 333-336.

V, K. P., A. G, R., & U, S. (2021, 3-5 Dec. 2021). *Design Optimization of Polymeric Insulators Under Various Environmental Conditions.* Paper presented at the 2021 IEEE 5th International Conference on Condition Assessment Techniques in Electrical Systems (CATCON).

Vancia, B., Saha, T., & Gillespie, T. (2005). *Electric Field Modelling of Non-Ceramic High Voltage Insulators*.

Vancia, B., Saha, T.K. and Gillespie, T. (2001). *Electric field modelling of non-ceramic high voltage insulators.* Phd Thesis, University of Queensland.

Wan, S., Liu, Z., Cao, W., Gu, S., Liu, X., & Du, X. (2020, 6-10 Sept. 2020). *Influence of UHV DC Transmission Line Arrester on Electric Field Distribution of Composite Insulator.* Paper presented at the 2020 IEEE International Conference on High Voltage Engineering and Application (ICHVE).

Weida, D., Steinmetz, T., & Clemens, M. (2008, 27-31 May 2008). *Electro-Quasistatic High-Voltage Field Simulations of Insulator Structures Covered with Thin Resistive Pollution or Nonlinear Grading Material.* Paper presented at the 2008 IEEE International Power Modulators and High-Voltage Conference.

Weiguo, Q., & Sebo, S. A. (2001, 18-18 Oct. 2001). *Electric field and potential distributions along non-ceramic insulators with water droplets.* Paper presented at the Proceedings: Electrical Insulation Conference and Electrical Manufacturing and Coil Winding Conference (Cat. No.01CH37264).

Weiguo Que, S. A. S. (2001). *Electric field and potential distributions along non-ceramic insulators with water droplets.* Electrical Insulation Conference and Electrical Manufacturing and Coil Winding Conference, 441-444.

Yan, C., Chen, J., & Ma, Y. (2019, 24-25 Aug. 2019). *Grey Wolf Optimization Algorithm with Improved Convergence Factor and Position Update Strategy.* Paper presented at the 2019 11th International Conference on Intelligent Human-Machine Systems and Cybernetics (IHMSC).

Yang, W., Zhu, T., Tian, Y., Zhu, S., & Yang, X. (2020). *Computation and Analysis of Electric Field Distribution Under Lightning Impulse Voltage for 1000-kV Gas-Insulated-Switchgear Spacer.* Journal of Electrical Engineering & Technology, 15(4), 1745-1758.

Yu, H., Yu, Y., Liu, Y., Wang, Y., & Gao, S. (2016). *Chaotic grey wolf optimization.* Journal of Computational Design and Engineering Volume 5, Issue 4.

Zhang, Y., Wang, Y., & Peng, C. (2009, 25-27 Dec. 2009). *Improved Imperialist Competitive Algorithm for Constrained Optimization.* Paper presented at the 2009 International Forum on Computer Science-Technology and Applications.

Zhao, T., & Comber, M. G. (2000). *Calculation of electric field and potential distribution along nonceramic insulators considering the effects of conductors and transmission towers.* IEEE Transactions on Power Delivery, 15(1), 313-318.

Zheng, J. C., Wang, Z., & Liu, Y. W. (1993, 19-21 Oct. 1993). *Influence of humidity on flashover in air in the presence of dielectric surfaces.* Paper presented at the Proceedings of TENCON '93. IEEE Region 10 International Conference on Computers, Communications and Automation.